

This is an Open Access document downloaded from ORCA, Cardiff University's institutional repository: <https://orca.cardiff.ac.uk/id/eprint/158264/>

This is the author's version of a work that was submitted to / accepted for publication.

Citation for final published version:

Palmer, Paul I., Wainwright, Caroline M. , Dong, Bo, Maidment, Ross I., Wheeler, Kevin G., Gedney, Nicola, Hickman, Jonathan E., Madani, Nima, Folwell, Sonja S., Abdo, Gamal, Allan, Richard P., Black, Emily C. L., Feng, Liang, Gudoshava, Masilin, Haines, Keith, Huntingford, Chris, Kilavi, Mary, Lunt, Mark F., Shaaban, Ahmed and Turner, Andrew G. 2023. Drivers and impacts of Eastern African rainfall variability. *Nature Reviews Earth & Environment* 10.1038/s43017-023-00397-x

Publishers page: <http://dx.doi.org/10.1038/s43017-023-00397-x>

Please note:

Changes made as a result of publishing processes such as copy-editing, formatting and page numbers may not be reflected in this version. For the definitive version of this publication, please refer to the published source. You are advised to consult the publisher's version if you wish to cite this paper.

This version is being made available in accordance with publisher policies. See <http://orca.cf.ac.uk/policies.html> for usage policies. Copyright and moral rights for publications made available in ORCA are retained by the copyright holders.



Physical drivers and multifarious impacts of Eastern African rainfall variations

Paul I. Palmer^{1,2†}, Caroline M. Wainwright³, Bo Dong^{4,5}, Ross I. Maidment⁴, Kevin G. Wheeler⁶, Nicola Gedney⁷, Jonathan E. Hickman^{8,9}, Nima Madani^{10,11}, Sonja S. Folwell¹², Gamal Abdo¹³, Richard P. Allan^{4,5}, Emily C. L. Black⁴, Liang Feng^{1,2}, Masilin Gudoshava¹⁴, Keith Haines^{4,5}, Chris Huntingford¹², Mary Kilavi¹⁵, Mark F. Lunt¹, Ahmed Shaaban^{16,17} and Andrew G. Turner⁴

1) School of GeoSciences, University of Edinburgh, Edinburgh, UK;

2) National Centre for Earth Observation, University of Edinburgh, Edinburgh, UK;

3) Grantham Institute, Imperial College London, London, UK;

4) Department of Meteorology, University of Reading, Reading, UK;

5) National Centre for Earth Observation, University of Reading, UK

6) The Environmental Change Institute, University of Oxford, Oxford, UK;

7) Met Office Hadley Centre, Joint Centre for Hydrometeorological Research, Wallingford, UK;

8) Center for Climate Systems Research, Columbia Climate School, Columbia University, New York, NY, USA;

9) NASA Goddard Institute for Space Studies, New York, NY, USA;

10) UCLA Joint Institute for Regional Earth System Science and Engineering, CA, USA;

11) Jet Propulsion Laboratory, Pasadena, CA, USA;

12) UK Centre for Ecology and Hydrology, Wallingford, UK;

13) Department of Civil Engineering, University of Khartoum, Khartoum, Sudan;

14) IGAD Climate Prediction and Applications Centre, Nairobi, Kenya;

15) Kenya Meteorological Department, Nairobi, Kenya;

16) Department of Atmospheric and Environmental Sciences, University at Albany, State University of New York (SUNY), Albany, NY, USA;

17) Egyptian Meteorological Authority, Cairo, Egypt.

† email: paul.palmer@ed.ac.uk

Abstract

Eastern Africa experiences extreme rainfall variations that have profound socio-economic impacts. In this Review, we synthesize understanding of observed changes in seasonal regional rainfall, its global to local forcings, the expected future changes and the associated environmental impacts. We focus on regions where annual bimodal rainfall is split between long rains (March-May) and short rains (October-December). Since the early 1980s, the long rains have got drier (-0.13—1.23 mm/season/decade) although some recovery is observed in 2018 and 2020. Meanwhile, the short rains have got wetter (1.27—2.58 mm/season/decade). These trends, overlaid by substantial year-to-year variations, impact the severity and frequency of extreme flooding and droughts, the stability of food and energy systems, the susceptibility to water-borne and vector-borne diseases and ecosystem stability. Climate model projections of rainfall changes vary but there is some consensus that a warming climate will increase rainfall over Eastern Africa. Climate models suggest that by 2030-2040 the short rains will deliver more rainfall than the long rains, which has implications for sustaining agricultural yields and triggering climate-related public health emergencies. Mitigating the impacts of future Eastern African climate requires continued investments in agriculture, clean water, medical and emergency infrastructures that are commensurate to the upcoming existential challenges.

49
50
51
52
53
54
55
56
57
58
59
60
61
62
63
64
65
66
67
68
69
70
71
72
73
74
75
76
77
78
79
80
81
82
83
84
85
86
87
88
89
90
91
92
93
94
95

Key points [30 words or fewer]

- Rainfall across Eastern Africa is changing rapidly with future projections suggesting these changes will continue, driven by increasing atmospheric greenhouse gases and by greater natural variability of the climate system.
- Within the 2030-2040 timeframe, climate models suggest that the short rains will deliver more rainfall over Eastern Africa than the long rains, subject to caveats, that has traditionally supported agriculture.
- During the 2030-2040 period, climate models suggest a higher frequency and severity of droughts that are also associated with significant humanitarian and socio-economic impacts.
- Projected rainfall changes will lead to widespread changes in agricultural yields and accessibility to clean water that will further increase the risk of food and water insecurity across Eastern Africa.
- Future rainfall changes will result in multifarious and long-term costs to human health and wellbeing, and the urban and natural environments.
- Development of adaptation strategies to improve agricultural yields and access to clean water, and to prepare for vector-borne disease outbreaks, will help avoid an unprecedented-scale public health emergency.
- Targeted improvements to meteorological observing systems will help improve the quality of meteorological forecasts over Eastern Africa that enable early warning systems to deliver better actionable information to individual countries

Introduction

Seasonal rainfall is integral to the 457 million people living across Eastern Africa, a region including Somalia, Burundi, Djibouti, Ethiopia, Eritrea, Kenya, Rwanda, South Sudan, Sudan, Tanzania and Uganda (**Box 1**). The number, duration and timing of these seasons varies across the region, driven principally by the movement of the intertropical convergence zone (ITCZ)¹. For instance, the most northern and southern countries (northern Ethiopia, Eritrea, Sudan, South Sudan and southern Tanzania) experience a single summer wet season for their respective hemisphere. In contrast, countries between these latitudinal extremes (encompassing Kenya, Uganda, Somalia, Burundi, Rwanda and parts of northern Tanzania and southern Ethiopia) experience two wet seasons. These two wet seasons occur during boreal spring (typically March-May, MAM; the more intense long rains) and autumn (typically October-December, OND; the less intense short rains), although there are substantial regional variations in these timings. We focus mainly on countries that have annual bimodal rainfall.

This seasonal rainfall is vital to the health and economic prosperity of the region. For example, long rains support agricultural production and thus national food security. Rain-fed agriculture, in turn, has a substantial role in the economy of many Eastern African countries. Agriculture employs 67% of people in Ethiopia, 80% in Somalia, 54% in Kenya, 63% in Eritrea and 38% in Sudan (data taken from World Bank Open Data). Agriculture also represents a substantial contribution to the annual multi-billion-dollar export of goods such as sugar, tea, coffee, tobacco, nuts and seeds, cut flowers and vegetables (taken from the Observatory of Economic Complexity). Moreover, rainfall is pivotal to energy production, particularly given that

96 hydropower represents a substantial fraction of electricity generation in Eastern Africa².
97 Aquifer recharge from rainfall^{3,4} also provides a sustainable reservoir of groundwater for
98 potable water (and irrigation) during periods of drought³, demonstrating the importance of
99 rainfall for water security, especially when looking to the future⁵.

100
101 Observed rainfall variability, particularly the disruption to the long and short rains, can
102 therefore result in a wide range of humanitarian, economic and environmental impacts. For
103 example, three anomalously low rain seasons over Somalia from April 2016 to December
104 2017 resulted in sustained and widespread drought conditions that led to significant losses of
105 agricultural crops and livestock⁶. Consequently, more than six million people faced acute food
106 shortages and malnutrition⁷, exacerbated by a shortage of potable water that led to disease
107 outbreak. A similar situation is unfolding in 2022 (ref ^{8,9}), with poor rain seasons since late
108 2020. In stark contrast, consecutive anomalously high rain seasons over South Sudan since
109 2019 has led to prolonged flooding, affecting more than 800,000 people¹⁰. Recurrent flooding
110 has damaged water treatment facilities, leaving millions without potable water, resulting in the
111 outbreak of cholera and diseases spread by mosquitoes. Fields that typically support
112 subsistence farming are submerged by floodwater, leading to a significant reduction in land to
113 cultivate. This situation is exacerbated by conflict¹⁰. As such, there are concerns over
114 widespread disruptions to clean sources of energy², depletion of surface and groundwater
115 reservoirs¹¹, devastating flooding events¹², and reductions in agricultural crop yields¹³ and
116 livestock productivity¹⁴. To help mitigate such impacts and inform future adaptation changes,
117 it is therefore vital to fully understand all aspects of Eastern African rainfall impacts, particularly
118 in light of continued changes arising from anthropogenic warming¹⁵.

119
120 In this Review, we synthesize the literature regarding observed rainfall variations over Eastern
121 Africa, focused on regions with a bimodal rainfall season, and their physical drivers. We
122 subsequently outline the economic, humanitarian and environmental impacts of such
123 observed rainfall variability. Based on state-of-the-art climate model projections, we also
124 describe the major climatological changes anticipated for Eastern Africa, and the associated
125 likely future impacts. Finally, we identify key gaps in knowledge and how these can be
126 addressed in future research.

127 128 **2 Drivers of Eastern African rainfall**

129
130 The timing and magnitude of the seasonal cycle of rainfall varies across Eastern Africa (**Fig.**
131 **1**). A single peaked seasonal cycle is evident over the majority of the Nile basin during June-
132 August, whereas two distinct rainfall seasons (short rains and long rains) are observed over
133 the Juba-Shabelle and northeast coast basins; some combination of the two occur over the
134 Rift Valley basin and the Central-East coast basin.

135
136 There are substantial seasonal and interannual variations in rainfall totals (**Fig. 1**). For
137 example, the standard deviation of rainfall over the Nile Basin during August (typically the
138 wettest month) is 17 mm month⁻¹, representing ~12% of the long-term August mean rainfall
139 according to the GPCC dataset. Whereas across the Juba-Shabelle Basin, rainfall is
140 considerably more variable. The standard deviation is 36 mm month⁻¹ during the peak of the
141 long-rains (April) and 52 mm month⁻¹ during the peak of the short-rains (October), representing
142 30% and 60% of their long-term means, respectively. The variability over the Juba-Shabelle
143 Basin during October is such that extremes between 1983-2019 have been recorded with a

144 minimum of just 34 mm month⁻¹ in 2003 (39% of the long-term mean) and a maximum of 305
145 mm month⁻¹ in 1997 (355% of the long-term mean). This variability is driven by various local
146 and remote physical processes, which we now discuss.
147

148 **2.1. Global teleconnections**

149 Rainfall variability over Eastern Africa is influenced by a range of global and regional modes
150 of climate variability (**Fig. 2**), including the El Niño Southern Oscillation (ENSO), the Indian
151 Ocean Dipole (IOD), the Quasi-Biennial Oscillation (QBO) and the Madden-Julian Oscillation
152 (MJO).

153 The IOD is a key driver of interannual variability across Eastern Africa during the short rains.
154 The positive phase of the IOD is defined by sustained positive SST anomalies in the western
155 Indian Ocean (50°E-70°E, 10°S-10°N) and negative SST anomalies in the eastern Indian
156 Ocean (90°E-110°E, 10°S-0°S), resulting in an SST difference between the two that exceeds
157 +0.4°C. The positive IOD is linked with wetter short rains over Eastern Africa (**Fig. 2**), with
158 precipitation totals that can be 2-3 times the long-term mean¹⁶, as seen in 1997, 2006, 2012,
159 2015 and 2019. The negative IOD, defined by a sustained SST difference <-0.4°C, is
160 associated with weaker short rains¹⁷, resulting in 20-60% of the long-term mean rainfall.

161 Links between ENSO and Eastern African short rains are also apparent¹⁸. East Pacific and
162 central Pacific El Niño events typically result in wetter short rains over Eastern Africa, and La
163 Niña conditions result in drier short rains¹⁹ (**Fig. 2**). However, the ENSO impact on Eastern
164 Africa is strongly mediated by the IOD¹⁸. The typical concurrence of positive IOD with East
165 Pacific El Niño, and negative IOD with East Pacific La Niña, act to amplify precipitation
166 responses, resulting in even larger anomalies across the region. For instance, the
167 coincidence of the 1997 El Niño with a strong positive IOD event led to rainfall anomalies twice
168 the climatological mean values over the short rains season¹⁶. In contrast, the strong central
169 Pacific El Niño of 2015 coincided with a weaker IOD, producing anomalies ~50% above the
170 climatological mean¹⁸. However, these relationships are non-linear, as demonstrated by
171 extreme 2019/2020 rainfall that occurred during an anomalously positive phase of the IOD but
172 neutral ENSO conditions²⁰.

173 The IOD and ENSO physically influence Eastern African rainfall by modifying the Indian Ocean
174 Walker Circulation (**Fig. 2**). In the absence of a strong phase of ENSO and IOD during the
175 rainy season, the Indian Ocean Walker Circulation consists of a strong upward branch over
176 the western Pacific warm pool and a much weaker updraft over Eastern Africa. However, when
177 there are unusually warm SSTs over the western Indian Ocean and central Pacific and
178 unusually cool SSTs over Southeast Asia (a positive IOD and El Niño conditions), the Indian
179 Ocean Walker Circulation weakens^{21,22}; a strong branch of rising air occurs over the western
180 Indian Ocean and a strong branch of sinking air over the western Pacific. This circulation
181 pattern is associated with elevated rainfall over Eastern Africa. A concurrent positive IOD and
182 El Niño event reinforces these impacts, leading to enhanced rainfall anomalies during short
183 rains over Eastern Africa¹⁸.

184 Strong El Niño events can lead to warmer SSTs in the Western Pacific (sometimes referred
185 to as a “Western V Pattern”²³). Warmer SSTs in the western equatorial Pacific are linked to

186 drier short rains over Eastern Africa and warmer SSTs in the western North Pacific are
187 associated with dry conditions during the long rains. Warmer SSTs over the western North
188 Pacific strengthen the Walker Circulation that suppresses Eastern African long rains. This SST
189 pattern led to successive dry seasons and droughts across Eastern Africa during 2016-2017
190 (ref²³). Variations in the long rains are less sensitive to changes in IOD²⁴, since the IOD peaks
191 several months later (during September-November) than the peak in the long rains.

192
193 The pan-tropical MJO is a further driver of sub-seasonal rainfall variability over Eastern Africa,
194 influencing both the long and short rains on a monthly basis²⁵. The MJO is described in terms
195 of eight phases, corresponding to locations of elevated convection (and rainfall). For example,
196 MJO phases 2-4 are linked with large-scale convection in the Indian Ocean, resulting in
197 westerly wind anomalies and enhanced rainfall¹⁸ (including 22%-78% of extreme rainfall
198 events, depending of MJO phase and amplitude²⁶) over the Eastern African highlands²⁶⁻²⁸
199 (**Box 1**). This relationship is weaker in October and April than in November, December, March
200 and May²⁹. In contrast, MJO phases 6-8 are associated with suppressed convection across
201 Eastern Africa and the western Indian Ocean, but wet conditions over low-lying coastal
202 regions^{26,27}. Greater seasonal rainfall accumulations are observed during a long rains season
203 when the MJO is more active in any phase³⁰, with the MJO explaining ~20% of the observed
204 interannual rainfall variations.

205
206 Through its relationship with the MJO³¹, the eastward phase of the QBO also influences
207 Eastern African rainfall. Above average long rains are linked to an easterly QBO in the
208 preceding September-November³⁰. This six-month lag³², is consistent with the time scale
209 associated with the descent of mid-stratospheric wind anomalies to the tropopause³³. The
210 QBO typically explains <20% of observed interannual rainfall variations, and the strength of
211 this lagged correlation is dependent on which model reanalysis is used³⁴, due to model-
212 specific assumptions about convective parameterizations.

214 **2.3. Local drivers of variability**

215 Variations in Indian Ocean SSTs, particularly those in the west that are partially controlled by
216 the IOD³⁰, are also linked with variability in both rainy seasons. Warmer SSTs heat the
217 boundary layer leading to anomalous ascent, opposing the climatological subsidence and
218 corresponding drying, thereby enhancing rainfall. Positive SST anomalies in the western
219 Indian Ocean increase the magnitude of short rains over 95% of equatorial Eastern Africa³⁵,
220 and explain 9-26% of observed rainfall variations during the long rains³⁰. The positive
221 correlation between western Indian Ocean SSTs and rainfall is strongest at the beginning and
222 end of the long rains season³⁶ when the rainfall is less well established and more susceptible
223 to local and remote forcing. Rainfall during the peak of the long rains (April) is also significantly
224 correlated with southern Atlantic SSTs, whereby cooler SSTs lead to higher rain rates over
225 Kenya driven by zonal winds over central Africa³⁶.

226 The presence of tropical cyclones in the southwest Indian Ocean (when the MJO is in phases
227 3-4) is associated with low-level westerly anomalies over Eastern Africa, resulting in enhanced
228 rainfall³⁷. There is a greater likelihood of westerly flow when the cyclones are located to the
229 east of Madagascar²⁸. The cyclone locations and rainfall impacts over Eastern Africa in 2018
230 and 2019 are consistent with this west/east pattern^{37,38}. Cyclones Dumazile and Eliakim in

231 2018 were located east of Madagascar and were associated with westerly flow and enhanced
232 rainfall, while Cyclone Idai in 2019 was located west of Madagascar and coincided with a drier
233 period^{37,38}.

234 The influence of the Congo airmass, characterized by the 700hPa zonal winds, has also been
235 associated with interannual variability of the long rains^{28,36}. Despite climatological easterly
236 winds, westerly winds originating from the Congo sometimes occur during March-May (often
237 linked to phase 3-4 of the MJO²⁸), bringing moist air that leads to convergence around Lake
238 Victoria and enhances rainfall^{28,36}. Indeed, the cumulative rainfall total of the long rains is
239 further strongly correlated with 700hPa zonal winds across the Congo Basin and Gulf of
240 Guinea. Furthermore, enhanced surface westerlies from the Congo basin, driven by a higher
241 geopotential height gradient over the Congo Basin than the western Indian Ocean, lead to
242 wetter long rains over Tanzania³⁹.

243 **3 Observed changes in Eastern African rainfall**

244
245 In addition to interannual variability driven by remote and local drivers, precipitation across
246 Eastern Africa also exhibits decadal-scale trends. Since the early 1980s, a range of satellite-
247 derived rainfall data products have helped to quantify these changes^{40,41} (**Fig. 3**). These data
248 products show consistent wetting trends over the Ethiopian highlands (5–12°N, 34–38°E)
249 during March-May (long rains) and the Horn of Africa (2°S–8°N, 35–51°E) during October-
250 December (short rains), with ranges across different datasets of 0.3-1.7 mm season⁻¹ year⁻¹
251 and 1.7-2.7 mm season⁻¹ year⁻¹, respectively (**Fig. 3a, b**). Elsewhere in Eastern Africa,
252 however, rainfall trends based on satellite data are inconsistent in magnitude and sign during
253 both rainy seasons, with the largest discrepancies between data products over the eastern
254 Congo Basin (**Fig. 3a, b**).

255
256 In addition to discrepancies between satellite datasets, substantial differences between
257 satellite products and gauge-based records over Eastern Africa add to the uncertainty in
258 estimating long-term spatially resolved seasonal rainfall trends (**Fig. 3c, d**). For example, while
259 satellite records reveal statistically significant trends, gauge-based records, available from the
260 1950s to 2018, do not display significant trends in precipitation or streamflow⁴². These
261 differences arise from contrasting satellite rainfall estimation methodologies, and spatial and
262 temporal gaps in the rain gauge network^{43,44}. However, there is better agreement between
263 areal-weighted rainfall means from different data products in both rainy seasons (**Fig. 3c, d**),
264 particularly after year 2000 when there are fewer gaps in the satellite records⁴⁵, resulting in
265 greater confidence in reported rainfall trends particularly for both the long and short rains.

266 **3.1. Long rains**

267
268 Over Eastern Africa, consistent negative long rain trends were observed over 1985-2010 (**Fig.**
269 **3a, c**). The magnitude of these trends is sensitive to the dataset used, ranging from -0.7 mm
270 season⁻¹ year⁻¹ to -1.5 mm season⁻¹ year⁻¹. Particularly marked declines occurred in ~1999
271 and 2010-2011 (refs⁴⁶⁻⁴⁹), the latter event causing devastating droughts in Kenya, Somalia
272 and south-eastern Ethiopia. Trends calculated up until ~2017 also continue to be negative.
273 However, very wet long rains in 2018 and 2020 indicate some recovery (**Figure 3a, c**). Trends
274 computed between 1983-2021 therefore no longer indicate widespread and consistent drying
275 across the Horn of Africa. Instead, less consistency emerges among datasets (**Fig. 3a, c**),

276 with some indicating a general wetting trend (TAMSAT, 1.23 mm season⁻¹ yr⁻¹; 0.47% season⁻¹
277 yr⁻¹) and others an overall drying trend (GPCC, -0.13 mm season⁻¹ yr⁻¹; -0.08% season⁻¹ yr⁻¹)
278 when considering the period 1983-2019.

279 Different mechanisms have been proposed to explain this reduction in the long rains up to the
280 2010s. On the one hand, the decline has been linked to Pacific Ocean SST variability⁵⁰⁻⁵².
281 Specifically, Pacific Decadal Variability manifests as a pattern of SST that has a larger
282 latitudinal extent than associated with ENSO, and has been described as a “Western V”
283 pattern that encapsulates warm SST values centred over the western Pacific warm pool with
284 tongues of warm SSTs extending northeastward toward Hawaii and southeastward into the
285 southern central Pacific^{23,53}. Warming of Indo-Western Pacific SSTs enhances convection
286 over the western equatorial Pacific leading to an anomalous Walker circulation over the Indian
287 Ocean, strengthening of the upper-level easterlies, increased subsidence over Eastern Africa
288 in the descending branch, and consequently reduced rainfall during the long rains^{54,55}. In some
289 instances, the strengthening of the upper-level easterlies has been highlighted as the
290 dominant driver in this process, with minimal connections to Walker Circulation variability⁵⁵.
291 More rapid warming of the West Pacific relative to the East Pacific since 1998, associated with
292 a negative phase of the Pacific Decadal Oscillation⁵⁶, has been linked with a greater
293 susceptibility of the long rains to drought during La Niña events with an increased risk of
294 concurrent short-long rains droughts²³. Strengthening of the W-E SST gradient across the
295 Pacific since 1998 has led to a stronger Walker circulation and faster Pacific trade winds^{57,58}
296 that results in drying over Eastern Africa via Indian Ocean teleconnection, in contrast with
297 coupled climate model simulations⁵⁹.

298 On the other hand, the shortening of the long rains season⁴⁷ (later onset and earlier cessation)
299 from the 1980s to late 2000s has been attributed to the rainfall decline. In this case, faster
300 SST warming in the Arabian Sea compared to further south, enhances the pressure gradient
301 and thus a faster-moving rainband. Declining westerly 700 hPa winds are also linked with the
302 decadal drying trend during the long rains⁴⁸, driven by changes in geopotential height gradient
303 that are associated with increased heating around Arabia and the Sahara⁴⁸. Positive
304 anomalies in westerly winds are associated with enhanced rainfall over Eastern Africa (section
305 2.3) and conversely declining westerlies are associated with reduced rainfall. Finally, internal
306 variability^{47,48}, such as variations in SST that are not linked with radiative forcing, is also
307 thought to be a driver.

308 **3.2 Short rains**

309 Compared to the long rains, there is greater consistency in the sign and magnitude of short
310 rain trends (**Fig. 3b, d**). Trends calculated over 1983-2021 are broadly consistent across
311 CHIRPS and TAMSAT, each highlighting an increase in short rain totals of 50-100 mm. We
312 do not report the trend for GPCC because it is not available beyond 2019 but it is consistent
313 with CHIRPS and TAMSAT for the shorter period of 1983-2019. We also do not report the
314 trend for ARC because it includes spurious time-varying jumps⁴³ that compromise a robust
315 estimate for the trend. Spatially, all datasets exhibit this increasing rainfall trend over large
316 parts of Tanzania, Uganda, Kenya, Somalia and Ethiopia (**Fig. 3b**), ranging 1.27—2.58 mm
317 season⁻¹ year⁻¹ (0.92—1.82% season⁻¹ year⁻¹).

318
319 As with the long rains, regional-mean long-term linear trends in short rains are punctuated
320 with periods of anomalous rainfall. For example, short rain totals during 1997-1998 and 2019-

2020 were 2-3 times higher than climatological values¹⁶, the former being linked to the El Niño event^{49,60} and corresponding connections to the positive IOD, with the largest positive rainfall anomalies of 100-250 mm year⁻¹ reported in 1997, 2006, 2012, 2015, and 2019 (**Fig. 3d**). This is consistent with earlier analyses^{51,52} and with mechanisms that determine year to year variations.

We find that including 2020 and 2021 does not change the spatial pattern of rainfall changes during OND but does increase the magnitude of the wetting trend in the short rains, as it does for the long rains. In general, we find that the regional-mean wetting trend is mostly a result of short-term variability driven by changes in ENSO and the IOD.

3.3 Anthropogenic connections

Large year-to-year variability in the long and short rains discussed in the previous section presents a difficulty in interpreting drivers and isolating the anthropogenic imprint. Paleoclimate reconstructions provide a longer-term view of rainfall changes over Eastern Africa. They show that changes in rainfall in the last century across the globe are not unprecedented in the context of the past two millennia, but the rate at which rainfall is changing is unusual. These data reveal a drying trend over the past two centuries⁵⁰ and a recent increase in drought frequency over the Horn of Africa during March-May⁶¹.

Greenhouse gas-induced warming drives an increase in atmospheric moisture and its convergence which intensify wet seasons while higher temperatures and greater evaporative demand intensify dry seasons, contributing to a greater severity of wet and dry extremes⁶². Cooling from anthropogenic aerosols has partially offset these greenhouse gas changes, and, through an additional altered global distribution of aerosol forcing, have been implicated in a southward shift in the African ITCZ from the 1950s to the 1980s (ref ⁶³). Recovery from this altered state has been attributed to a combination of greenhouse gas and aerosol forcing⁶⁴. While there is some consensus about the human influence on rainfall over Eastern Africa (via greenhouse gas induced warming and cooling from anthropogenic aerosols^{21,64,65}), the anthropogenic influence on the physical processes (specifically the IOD) that control year-to-year rainfall changes is less clear^{55,66}. Based on a combined model and data analysis, drought trends over Eastern Africa are most consistent with changes in precipitation rather than increasing temperature⁶⁷.

An increased frequency of the positive phase of the IOD during the second half of the twentieth century has not led to higher seasonal rainfall amounts compared to the first half of the twentieth century⁵⁵. This observation is consistent with understanding of how a warming climate perturbs the thermal structure of the atmosphere and the circulation of the tropical oceans^{68,69}, resulting in a long-term weakening of Walker and Hadley circulations and the narrowing of the ITCZ^{55,70,71}. Yet, observed strengthening of the Walker circulation since the 1990s, associated with rapid warming of the tropical west Pacific relative to the east Pacific, is not reproduced well by simulations and this has been linked with systematic model biases that may limit the projections of Eastern African rainfall⁵⁹. Therefore, anthropogenic signals of Eastern Africa rainfall are yet to be clearly established in the observational record and future projections assessed in Section 5 should be interpreted in the context of these complex present-day drivers and uncertainties.

4 Impacts of observed rainfall variations

Local and remotely driven variability in the short and long rains have substantial and multifarious environmental, humanitarian and economic impacts occurring over various temporal scales. Given the diversity of the impacts of Eastern African rainfall variability, we focus here on three broad groupings of impacts: agriculture, natural ecosystems, water security, and human health. These impacts are not exhaustive but represent a diverse subset of widely researched topics. It is also important to bear in mind that precipitation impacts do not occur in isolation; often such impacts coincide with changes in temperature, complicating explicit attribution to rainfall.

4.1. Agricultural impacts

Rainfall variability across Eastern Africa affects agriculture directly and indirectly. Much agriculture in the region is rain-fed. As such, failure of seasonal rains result in agricultural droughts, the frequency of which has increased from once every ten years in the early 1900s to once every three years since 2005 (ref⁷²). While small- and large-scale irrigation schemes are helping to mitigate the impacts^{73,74}, minimal infrastructure exists to retain, redistribute and store water to cope with this intra-seasonal and interannual variability. The resulting loss of agricultural production has thus been the cause of some of the most well-known humanitarian disasters in the 20th and 21st centuries, including the 1974 Sahel drought which resulted in an estimated 325,000 deaths, and the 1984 drought across Ethiopia and Sudan that caused 450,000 deaths⁷⁵⁻⁷⁷. Since then, Ethiopia has experienced several droughts. One responsible factor is El Niño, which results in contrasting impacts over Ethiopia⁷⁸: lower than normal rainfall over northern Ethiopia that responds similarly to the Sahel region, and higher than normal rainfall over southern Ethiopia that can lead to flooding. Variations in the climate system, e.g., location of the ITCZ, and regional orography (**Box 1**) complicate this relationship.

The 1997/1998 drought over northern Ethiopia, while not as extreme or as widespread as the drought in 1984, illustrates other agricultural impacts. Cereal production⁷⁹ declined by 25% during this period, resulting in price increases of 15-45%. This was due to lower crop yields due to drought and indirectly by reduced cultivated land because of malnourished oxen⁸⁰. Reduced crops also caused cattle mortality rates of 26% in some regions due to dehydration/starvation and disease⁸¹, with cattle typically more affected by drought than camels or small ruminants⁸². Efforts to implement drought early-warning systems^{83,84} increase agricultural capacity by distributing drought-resistant seeds, and enhance rapid humanitarian responses from governments and international aid that seek (and have arguably helped) to mitigate deaths associated with food security^{85,86}. Humanitarian impacts of the historic drought⁸⁷ in 2015 and subsequent droughts⁸⁸ in Ethiopia and of the three major droughts over Somalia over the last decade (2011/2012, 2016/2017 and 2021/2022), due to consecutive failed rain seasons, demonstrate the complex and evolving challenges faced by Eastern African countries.

While below normal rainfall threatens agriculture, so does an increase in rainfall intensity. In regions that are moisture limited, benefits from increased rainfall can be expected⁸⁹. However, regions with low permeability soils such as the clay vertisols of the sub-humid regions of Ethiopia that have infiltration capacities of only 2.5 to 6.0 cm/day, the landscape is easily overwhelmed by intensive rainfall⁹⁰. Low permeability of irrigated lands results in waterlogging

417 and crop damage, and poor drainage systems substantially limit the production potential of
418 the soils⁹¹. For example, productivity losses of 45% over 60 years have been recorded for
419 some Ethiopian sugar plantations due to waterlogging. Furthermore, the erosion of agricultural
420 topsoil occurs when runoff from sloped terrain exceeds the rate of soil intake⁹², affecting future
421 productivity. An illustration of this is the unusually heavy rainfall over northern Ethiopia during
422 March and April 2016, immediately following extensive drought conditions, which led to
423 widespread flooding, landslides, displacement of people, and damage to crops. Based on
424 recent changes in rainfall over Eastern Africa, there is a growing influence of extreme rainfall
425 seasons that will continue to negatively impact agricultural productivity.

426
427 High densities of desert locusts (*Schistocerca gregaria*) also pose a threat to agricultural crops
428 and are strongly linked to rainfall variability. Heavy and extensive rainfall provides moist soil
429 for egg laying, and the subsequent rain-fed flushing of vegetation provides shelter and food
430 for the locusts causing widespread damage. As such, rainfall is a dominant factor governing
431 their population and movement, as evidenced by several documented locust plagues over
432 Eastern Africa^{93–96}. The extent of crop damage is related to successfully locating locusts
433 breeding grounds and to proactive interventions that are sometimes compromised by armed
434 conflict⁹⁷. Given rainfall connections to the IOD and ENSO, locust plagues and resulting crop
435 damage typically occur during positive IOD years when rainfall is enhanced⁹⁸, for example,
436 the years 1986/1987, 1992/1993, and 2019/2020. These remote drivers often interact with
437 local drivers. For example, the 2020 locust outbreak—the worst in 25 years for Ethiopia and
438 Somalia and in 70 years for Kenya—has been linked to the rare landfall of two tropical
439 cyclones in the Arabian Peninsula during 2018, exponential growth in breeding through the
440 creation of ephemeral lakes, their southward migration to Eastern Africa, and subsequent
441 establishment of the swarm from IOD-related enhanced vegetation growth. The COVID-19
442 pandemic along with other factors prevented proactive interventions in this case and resulted
443 in an estimated US\$8.5 billion in crop damage in Yemen and Eastern Africa during 2020,
444 amplifying threats to food security⁹⁹. Indeed, over Ethiopia between December 2019 and
445 March 2020, 114,000, 41,000 and 36,000 hectares of sorghum, maize and wheat were
446 estimated to be damaged¹⁰⁰, respectively.

447
448 SSTs prior to cyclogenesis have got progressively warmer over the north Indian Ocean¹⁰¹ over
449 the period 1980–2020, facilitating higher heat fluxes from the ocean to the atmosphere that
450 are linked to the frequency and intensity of cyclones. Generally, differential warming of SSTs
451 across the Indian Ocean affects the location of cyclogenesis. Particularly, there has been rapid
452 warming over the Arabian Sea and the Bay of Bengal thereby increasing the chances of the
453 storms reaching land and creating ephemeral lakes that can sustain locust breeding. Indeed,
454 three times the number of cyclones affected the Arabian Peninsula during the 2010s
455 compared with the previous two decades. The frequency of cyclones in the north Indian Ocean
456 is also linked with warmer SSTs over the eastern Indian Ocean associated with the negative
457 IOD pattern¹⁰².

458 459 **4.2 Ecosystem impacts**

460
461 Rainfall variability also has strong bearing on various ecosystem functions, including terrestrial
462 gross primary production (GPP), wildfire activity and wetland emissions of greenhouse gases.

464 Terrestrial GPP—the total amount of carbon fixed by plants—is closely related to water
465 availability in Eastern Africa’s tropical forest and savannah ecosystems¹⁰³. Tropical African
466 ecosystems are typically more limited by water than sunlight on a regional basis^{104,105}.
467 Interannual variations in water availability¹⁰³ through rainfall and groundwater result in GPP
468 variations within $\pm 10\%$ of climatological values. For forest ecosystems, GPP anomalies are
469 highly correlated with changes in groundwater and soil moisture, generally increasing during
470 periods of elevated rainfall, except in regions where annual rainfall exceeds 1800 mm¹⁰³. This
471 decline in productivity with higher rainfall may reflect reduced sunlight due to cloud cover. For
472 savanna ecosystems, rainfall patterns have a stronger influence on inter-annual variability in
473 productivity. Although, productivity in these ecosystems is also controlled by soil moisture and
474 groundwater because shrubs in dry savannas may still have access to below surface water¹⁰⁶
475 due to their deep rooting systems.

476
477 Much less is known about how African ecosystems respond to changes in rainfall than other
478 tropical ecosystems, but models of GPP driven by satellite observations of vegetative
479 properties, rainfall, and groundwater are beginning to improve our understanding. Based on a
480 GPP product¹⁰⁷ inferred from the NASA SMAP satellite instrument, the annual mean GPP for
481 2003-2017 is $\sim 3.08 \pm 0.19$ Pg/yr. Drought years of 2005 and 2015 and elevated rainfall in 2010
482 exemplify the range of GPP responses to rainfall changes that were driven by SST anomalies
483 in the South Atlantic and Indian Oceans. The weak El Niño year of 2005, immediately
484 preceded by years of anomalously low rainfall and depleted groundwater, led to a drop of 5%
485 in GPP over -5 - 10° N, 30 - 50° E (-0.15 Pg/yr). In contrast, in 2015 when there were similarly
486 weak El Niño conditions, anomalously low rainfall, particularly over latitudes -10 - 10° N, was
487 partially offset with groundwater reserves that were replenished in the preceding five years,
488 resulting in a GPP of 3.19 Pg/yr, close to the climatological mean value. During the strong
489 2010 El Niño, there were widespread increases in GPP across the region ($+0.15$ Pg/yr,
490 representing $+5\%$) except for parts of the Horn of Africa. Groundwater reservoirs can act as a
491 temporary buffer against drought during years of low rainfall for sufficiently deep rooting
492 systems, but only if they have an opportunity to replenish during anomalously wet years.
493 Regions that suffer from consecutive years of below average rainfall, such as countries in the
494 eastern most part of Horn of Africa, will see drops in GPP and eventually increasing rates of
495 vegetation mortality.

496
497 By influencing GPP, rainfall variability can also influence vegetation fire activity and
498 consequently emissions of air pollutants, CO₂ and other GHGs¹⁰⁸⁻¹¹⁰. For example, above
499 average rainfall during the growing season increases plant productivity, thereby increasing the
500 fuel load available for burning in subsequent seasons or years¹¹¹. In contrast, above average
501 rainfall during the dry season can suppress fire activity, although fire ignition via lightning is
502 enhanced during moist convection¹¹². Both processes have proven to be important in Eastern
503 Africa during initial years of the 21st century¹¹³.

504
505 Landscape fires in Eastern Africa are typically focused on South Sudan and parts of western
506 Ethiopia and northern Uganda during January and Tanzania and part of southern Uganda
507 during July. During the 2001-2012 period, changes in rainfall explained about 20% of the
508 negative trends in burned area in South Sudan¹¹⁴. Based on ENSO events during 1997-2016,
509 El Niño years lead to a small reduction in burned area anomalies in forest and non-forest
510 ecosystems over northern hemispheric Africa. Generally, ENSO plays a smaller role in burned

511 area and subsequent emissions than in other tropical biomass burning regions¹¹⁵. This is
512 supported by an ensemble analysis of Earth system models (ESMs)¹¹⁶.

513
514 Tropical wetland emissions of methane, an important greenhouse gas, exhibit marked
515 relationships with precipitation given the dominant control of inundation extent and water table
516 depth^{117,118}. Aquatic production of methane is due to anoxic decomposition of organic matter
517 from root systems and decaying plants, influenced by a range biochemical and phenological
518 factors^{119–121} and local macrophyte diversity^{122,123}.

519
520 Satellite data revealed the global significance of Eastern African wetland emissions of
521 methane over South Sudan and western Ethiopia during the long and short rain periods over
522 the last decade^{124–127}. Seasonal variations in emissions are controlled by local rainfall, whilst
523 longer-term changes are driven mostly by rainfall collected by upstream catchment areas (for
524 example, Lake Victoria, Lake Albert). Water released from these catchments is transported
525 downstream via the White Nile leading to demonstrable increases in wetland extent and
526 associated vegetation flushing, particularly over the Sudd^{128,129}. Wetland emissions from the
527 Sudd in South Sudan during 2010-2016 represented about a third of the global atmospheric
528 growth of methane. A strong positive phase of the IOD during 2018-2019 led to anomalously
529 large rainfall totals over Uganda and Kenya during March-May 2018 and October-December
530 2019, equivalent to a once in 30-year event¹³⁰. The additional methane emissions due to the
531 anomalous short rains in 2019, focused on South Sudan and Ethiopia, represented a quarter
532 of the global atmospheric methane growth rate for that year¹³⁰. The anomalous global
533 atmospheric methane growth rates in 2020 (ref^{131,132}) and 2021 (ref¹³²) have also been partly
534 attributed to anomalous Eastern African wetland emissions.

535
536 Wetlands can also be hotspots of ammonia (NH₃) gas emissions^{133,134}. Ammonia is a
537 precursor to the formation of secondary inorganic aerosols, which are the main contributor to
538 particulate matter globally and represents a hazard to human health^{135,136}, and its deposition
539 to downwind ecosystems can lead to eutrophication, soil acidification, reduced productivity,
540 biodiversity decline, and indirect GHG emissions^{137–140}. Ammonia is volatilized from
541 ammonium in soils via an abiotic reaction, which is influenced by pH, temperature, and, of
542 importance here, soil moisture content linked to changes in rainfall. When soils with high
543 moisture content start to dry out, NH₃-nitrogen tends to become more concentrated at the
544 same time as there are reduced limits on gas diffusion through soils, which, along with other
545 factors, leads to enhanced NH₃ emissions^{141–143}.

546
547 These processes have been shown to produce a large seasonal increase in NH₃
548 concentrations (8×10^{15} to 13×10^{15} molecules cm⁻²) over salt flats in Tanzania as the waters
549 of Lake Natron, a soda lake with relatively alkaline pH, recede during the dry season¹⁴⁴. A
550 similar seasonal behaviour has been observed over the Sudd wetlands in South Sudan¹⁴⁵.
551 Roughly half of the Sudd wetlands are permanently flooded, with part of the remaining wetland
552 area drying each year¹⁴⁶. The extent of drying can vary substantially from year to year. For
553 example, NH₃ concentrations over the region reached nearly 30×10^{15} molecules cm⁻² in 2010
554 when seasonal drying of the Sudd was most extensive, compared with 11×10^{15} molecules
555 cm⁻² in 2014 when drying was least extensive¹⁴⁵.

556 557 **4.3. Water security**

558
559
560
561
562
563
564
565
566
567
568
569
570
571
572
573
574
575
576
577
578
579
580
581
582
583
584
585
586
587
588
589
590
591
592
593
594
595
596
597
598
599
600
601
602
603
604

Rainfall variability has direct consequences for human wellbeing and health, including generation of clean energy from hydropower, transboundary water management, urban drainage, and vector-borne and water-borne diseases. A preliminary assessment by the UN in 2022 of water security across Africa¹⁴⁷, based on a range of ten criteria including access to drinking water, sanitation, and water infrastructure, highlighted that Eastern Africa includes some of the lowest scoring countries.

To meet growing energy demands in Eastern Africa, hydropower development is often seen as a viable solution and one that does not involve the combustion of fossil fuels. Ethiopia and Sudan seek to meet domestic energy needs and aspire to market energy across the East Africa Power Pool (EAPP). The current capacity of hydropower contributes about 50% of electrical generation in EAPP countries, with a planned doubling of capacity over Eastern Africa by 2030 that will mostly be in the Nile Basin. However, a strong dependency on hydropower places the entire economic system at the mercy of variable hydrologic conditions¹⁴⁸ in an increasingly uncertain climatic future^{149,150}. Linking energy networks across hydrologic zones and organising infrastructure investment to be ‘climate-proof’ is one potential solution, without which countries that rely heavily on hydropower will likely suffer from fluctuating electricity prices¹⁴⁸. The EAPP may help to coordinate the trade and interconnection of cross-border energy networks, but there remain significant political challenges as energy needs grow with projected future increases in urbanisation, expanding irrigation plans, and variable release from upstream hydropower plants^{148,151}.

While Zambia is not part of Eastern Africa it does serve as an example of the multiplicative consequences of rainfall variations on hydropower, and they are part of the southern African counterpart of the EAPP. Extremely dry conditions during 2015 and 2016 linked with the strong El Niño led to reduced inflow into Lake Kariba that feeds into the Kariba Dam that provides 1,830 megawatts of hydroelectric power to Zambia and Zimbabwe. Lake levels in January 2016 dropped to 12% of capacity, just above the minimum necessary to generate electricity¹⁵². This led to major energy deficit in Zambia that was managed by buying energy from neighbouring countries and daily power outages, particularly affecting Lusaka Province and the Copper Belt. This subsequently led to damages associated with a suspension of heating and refrigeration and, combined with a fall in global copper price, led to an estimated 19% drop in GDP¹⁵³. Conversely, anomalous flooding of the Zambezi basin due to torrential rainfall can overwhelm the Kariba Dam resulting in a necessary release of water. This occurred in March 2010 due to El Niño conditions, affecting the discharge rates of downstream dams, leading to major floods that impacted hundreds of thousands of people.

More generally, variability in precipitation presents an important issue for regional water security in Eastern African countries that include transboundary rivers¹⁵⁴. There are substantial challenges associated with managing critical multi-purpose infrastructures that support dams for hydropower but also for agricultural expansion and flood control, especially considering variations in rainfall and the associated river flows. Safely handling severe flooding and drought events requires close communication between managers of different dams, some of which will be across political borders, to avoid harm to co-riparian nations¹⁵⁵ and to avert international conflict¹⁵⁶.

605 Fortunately, violent conflict between nations over shared water resources is almost non-
606 existent anywhere on the globe¹⁵⁷. Over Eastern Africa, minor conflicts have been mainly led
607 by herders and farmers in neighbouring countries fighting over pasture and water for livestock.
608 Construction of the Grand Ethiopian Renaissance Dam (GERD) on the Blue Nile River has
609 the potential to be the biggest risk of conflict between neighbouring Eastern African
610 countries¹⁵⁵. The dam is part of Ethiopia's economic growth plan to become Africa's largest
611 hydropower exporter. However, there is concern that GERD will reduce downstream water for
612 irrigation and drinking, and to a lesser extent reduce hydropower capacity. Years of heavy
613 rainfall over Ethiopia, such as 2020, can help fill the GERD and result in release of sufficient
614 water to Sudan and Egypt¹⁵⁸. Proponents of GERD argue that in years with lower rainfall, the
615 dam's water storage can be used to alleviate drought in downstream countries. But this relies
616 on the dam releasing the water. Diplomatic negotiations are ongoing, but the situation serves
617 as an example of the complexities associated with transboundary water.

618

619 Economic development of Eastern African countries is tied to increasing urbanization,
620 resulting in rapid expansion of cities to accommodate growing populations¹⁵⁹. This includes
621 expansion of infrastructure to support access to electricity and clean water, removal of
622 wastewater and sewage treatment, development of road networks, and improved internet and
623 cellular connectivity. Periods of intense rainfall can quickly overwhelm inadequate
624 infrastructure¹⁶⁰, resulting in overflowing drainage systems, flooded houses and suspension
625 of sewage treatment that often leads to a range of health emergencies¹⁶¹. Flooding can also
626 damage roads and railways built with limited budgets and inadequate engineering, disrupting
627 the transportation of workers and food supplies from rural to urban areas and consequently
628 affecting economic activity¹⁶².

629

630 Heavy rainfall over Sudan in 2020 led to extensive flooding that damaged or destroyed
631 112,000 homes, causing a three-month state of emergency to be declared¹⁶³. Heavy rains and
632 flash flooding over Sudan in 2021 affected 88,000 people in 13 out of the 18 states. Damage
633 and destruction of houses and clean water sources were widespread. Flash flooding also
634 affected the sewage systems of internally displaced persons camps in South Darfur, closed
635 schools, power plant substations, and rendered roads impassable. The frequency and
636 magnitude of heavy rainfall across Sudan will continue to prove a challenge for urban areas
637 that do not have adequate infrastructure and will ultimately compromise the economic
638 development of the region.

639

640 **4.4. Human Health Impacts**

641

642 Rainfall is also a key component for the propagation of several vector-borne and water-borne
643 diseases relevant to Eastern Africa. The influence of temperature on the malaria parasite, for
644 example, is well understood^{164–166} compared to the impact of intense rainfall and associated
645 flooding on the mosquito life cycle and subsequent virus transmissions. Mosquitoes and other
646 arthropods that carry malaria and arboviruses such as dengue, often include an aquatic stage
647 to support the development of their eggs and larvae. A number of studies have focused on
648 extreme rainfall events during the El Niño phase of ENSO during 1997/1998 and
649 2015/2016^{167–170}. Other studies have linked the IOD to an increase in the risk of malaria in the
650 Eastern African highlands^{171,172}. There are similar challenges associated with water-borne
651 diseases such as cholera and typhoid that are prevalent across Eastern Africa, and become

652 of more concern during specific shifts in rainfall and variations in temperature^{162,173,174}.
653 Combatting these viruses is exacerbated by non-climate factors, including international travel,
654 pockets of increased population density associated with urbanisation, and land-use change
655 that can move peri-urban regions closer to mosquito and arthropod breeding grounds.

656

657 Extreme rainfall associated with the strong El Niño during 1997/1998 followed an extended
658 drought period and led to an outbreak of malaria in a non-immune population of north-eastern
659 Kenya, the extent of which had not been seen since 1952. Records of hospital admissions
660 reported a three-month lag after heavy rainfall in November 1997 (ref¹⁶⁷). Hospital data from
661 one community reported a ten-fold increase in expected daily rates of crude and under-five
662 mortality¹⁶⁷, which rapidly reduced by the end of April 1998 when rainfall subsided. A similar
663 story was reported for a district in western Uganda¹⁶⁸. For communities of the Tanzanian
664 highlands, however, researchers found a marked reduction in malaria cases in 1997/1998
665 compared to previous years. This reduction was attributed to flooding that can flush mosquito
666 larvae from breeding sites thereby decreasing the disease spread¹⁷⁵. Two out of the three
667 communities that reported an increase in malaria after the heavy rains were located next to a
668 body of standing water that is an ideal breeding ground for mosquitoes¹⁷⁵. More generally,
669 periods of heavy rainfall, irrespective of whether they are associated with El Niño or the IOD,
670 result in human health challenges for local communities that are overwhelmed by floods that
671 lead to pools of standing water^{169,170}.

672

673 We have described a few of the many impacts associated with rainfall extremes over Eastern
674 Africa. Trends and variations in rainfall are linked with, and therefore difficult to separate from,
675 changes in temperature. Concurrent changes in temperature^{176–178} can reinforce or weaken¹⁷⁹
676 impacts due to rainfall.

677

678 **5 Future changes**

679

680 Given the multifarious impacts of rainfall changes over Eastern Africa, there is a need to
681 consider how rainfall and its drivers might change in the future. This knowledge provides
682 actionable information with which to develop effective mitigation strategies.

683

684 *Rainfall*

685

686 Projected future changes in Eastern African climate have been studied using global and
687 regional climate models^{20,50,180–186} (GCMs and RCMs, respectively), each with considerable
688 spread amongst ensemble members and models, casting doubt on the reliability of
689 projections⁵⁹. Unfortunately, there are also limited relationships between the abilities of
690 individual models to describe past and future Eastern African climate and the model spread
691¹⁸⁷. Hence, constraining future projections simply by observation of current day ESM
692 performance is not possible.

693

694 These model limitations are particularly evident for the long rains when GCMs and RCMs
695 show substantial inter- and intra-model differences, resulting in a diversity of projected
696 responses and thus uncertainty. Indeed, GCMs report no significant change¹⁸⁴, a decrease¹⁸⁸
697 and a small increase in the long rains under anthropogenic warming, consistent with the range
698 of responses for CMIP5 models^{181,189}. CMIP6 simulations also exhibit variability, with the

699 multi-model ensemble providing hints of a small increase in the long rains for Eastern Africa
700 (the sum of IPCC southeast and northeast Africa regions) (**Fig. 4a**). Under Shared
701 Socioeconomic Pathway 2-4.5 (SSP2-4.5), for example, the multi-model median projects
702 statistically significant $0.02 \text{ mm day}^{-1} \text{ decade}^{-1}$ increases (2015-2100), although changes only
703 really emerge after ~ 2080 . These increases are also sensitive to the emission scenario used,
704 as demonstrated by a larger positive trend ($0.06 \text{ mm day}^{-1} \text{ decade}^{-1}$, 2015-2100) under SSP5-
705 8.5 (**Fig. 4b**), which also tend to emerge earlier (~ 2040). In contrast, CORDEX¹⁹⁰ regional
706 models support no such increase in the long rains, instead exhibiting a statistically significant
707 slight negative trend for Representative Concentration Pathway 4.5 (RCP4.5; $-0.01 \text{ mm day}^{-1}$
708 decade^{-1} , 2006-2100; **Fig. 4c**), and a statistically insignificant slight positive trend for RCP8.5
709 (**Fig. 4d**). Based on these calculations, there is no clear indication regarding the sign and
710 magnitude of future long rain changes over Eastern Africa, nor their potential drivers. These
711 minimal changes in long rains have been attributed to the continental thermal low, centred
712 near the equator and present during the long rains, being insensitive to changes in subtropical
713 atmospheric hydrodynamics driven by rising atmospheric GHG during the 21st century¹⁵.

714
715 These models generally exhibit better inter- and intra- model agreement for the short rains¹⁸¹,
716 albeit still with substantial spread, providing some confidence in the projected future climate
717 states. Indeed, the short rains are projected to increase with anthropogenic warming^{20,184,188}.
718 Under SSP2-4.5, the CMIP6 ensemble projects a statistically significant $0.04 \text{ mm day}^{-1} \text{ decade}^{-1}$
719 $(2015-2100)$ increase in the short rains, the increase emerging in the early 2040s (**Fig. 4a**).
720 These changes are more pronounced under SSP5-8.5 for the same period, wherein trends of
721 $0.11 \text{ mm day}^{-1} \text{ decade}^{-1}$ are projected, emerging earlier²⁰ in the 2030s (**Fig. 4b**). CORDEX
722 simulations exhibit a similar pattern: a small but statistically significant increase for RCP4.5
723 ($0.03 \text{ mm day}^{-1} \text{ decade}^{-1}$, 2006-2100; **Fig. 4c**), and a stronger response that emerges in the
724 late 2040s for RCP8.5 for the same period ($0.05 \text{ mm day}^{-1} \text{ decade}^{-1}$; **Fig. 4d**). A convection-
725 permitting regional model also supports these findings, additionally reporting a large increase
726 in extreme rainfall rates during the short rains¹⁹¹. The magnitude and large spatial extent of
727 this increase in extreme rainfall were underestimated by the corresponding regional models
728 using parametrised convection (including CMIP5, CMIP6 and CORDEX simulations) so they
729 may be underpredicting the full extent of future increases in rainfall intensity across Eastern
730 Africa¹⁹¹.

731
732 This increase in the short rains arises from increased moisture convergence over Eastern
733 Africa¹⁵. This enhanced moisture convergence emerges from increased atmospheric
734 moisture¹⁸⁴ due to a warming climate and from anomalous circulation patterns associated with
735 a strengthening in the continental low over southern Africa and the subtropical high over the
736 South Indian Ocean, and a weakening of the eastern Sahara subtropical high. A weakening
737 of the Walker circulation in response to warming SSTs over the western Indian Ocean also
738 favours an upward trend in the short rains^{50,188}. Nevertheless, limitations in model
739 representations of key processes and climatologies, for example, overestimates in the short
740 rains and underestimates in the long rains¹⁹², an unrealistic dominance of the Walker
741 circulation¹⁹³, and failure to reproduce the observed SST gradient across the equatorial
742 Pacific⁵⁹—all cast doubts on rainfall projections and understanding of their corresponding
743 drivers. With these caveats in mind, conclusions are limited to saying that the rainfall during
744 the short rains is increasing at a faster rate than the long rains (**Fig. 4**).

745
746 *ENSO and IOD*

747
748
749
750
751
752
753
754
755
756
757
758
759
760
761
762
763
764
765
766
767
768
769
770
771
772
773
774
775
776
777
778
779
780
781
782
783
784
785
786
787
788
789
790
791
792
793

ENSO and the IOD have had a dominant influence on rainfall variations across Eastern Africa. It is therefore instructive to understand their future projections in the hope of informing rainfall projections. As with rainfall itself, there is often a lack of consensus regarding how these modes of variability will change under anthropogenic warming. For ENSO¹⁹⁴, no significant change in intensity and frequency has been reported in some instances^{195–197}, while an increased occurrence of extreme El Niño and La Niña events is reported by others^{198–200}. Similarly, no significant change in the overall frequency and amplitude of the IOD is projected by coupled models^{201,202}, although the frequency of extreme positive IOD events is thought to increase^{198,203}. Assuming present-day relationships between Eastern African rainfall and ENSO and IOD remain the same in the future, the short rains would then become wetter with an increasing chance of torrential rains and associated higher risk of flooding, but also the potential for groundwater recharge⁴.

However, even if the frequency and intensity of ENSO and IOD do not change in a warming climate, there is some consensus about how these climatic modes of variability will remotely influence the future climate system. For instance, rainfall extremes associated with ENSO and IOD can be expected to be more severe in a warming world owing to an intensified hydrologic cycle²⁰⁴. Moreover, faster warming is expected in the western Indian Ocean compared to surrounding bodies of water^{198,201,205}. Because of these shifts, the tropical oceans will tend towards an El Niño-like and positive IOD-like state, associated with weakening of the Walker circulation, shifts in the ITCZ²⁰⁶ and an increase in atmospheric moist static energy. Consequently, as a result of changing background SSTs and circulation shifts during the short rains later this century, ENSO and IOD are expected to have a stronger coupling with rainfall over the Horn of Africa but a weaker coupling with rainfall over the southern part of Eastern Africa¹⁸⁸. The long rains, which are historically insensitive to remote SST forcing, would then become substantially more responsive to ENSO in future projections¹⁸⁸. Model projections also suggest an enhanced La Niña-related rainfall anomaly over Eastern Africa during July–September compared to the present period¹⁸⁸.

Uncertainty about future changes in ENSO and IOD, combined with potential changes in the strength of teleconnections results in considerable uncertainty around changes in future rainfall over Eastern Africa driven by ENSO and the IOD. If the frequency of extreme positive IOD events increases^{198,203}, and the strength of the teleconnection increases over the eastern part of Eastern Africa¹⁸⁸, this may result in wetter conditions over the eastern half of the region during the short rains. Changes in the frequency of El Niño and La Niña events, coupled with increasing sensitivity to ENSO during the long rains and summer rainfall seasons may lead to increasing variability in these seasons in the future. Additionally, increases in the frequency of extreme El Niño and La Niña events, and increasing teleconnection strength, may increase the frequency of extreme rainfall seasons throughout the year.

Impacts

As in the present climate, any future changes in seasonal rainfall across Eastern Africa will result in a wide range of economic and humanitarian impacts.

Changes in agricultural yields due to changing rainfall patterns are crop specific. Based on current understanding, future crop yields are more sensitive to uncertainties in temperature

794 than rainfall¹⁷⁷ due to crops generally having an optimal growing temperature range, outside
795 of which the yield falls off rapidly^{178,207}. Optimal yields also rely on adequate soil moisture that
796 helps to regulate available water in the plant root zone²⁰⁸. Changes in the timing, duration, and
797 magnitude of the long and short rains (Figure 4) will also need to be considered by farmers
798 when they decide which crops and seed-types are grown throughout the year²⁰⁹. Increased
799 frequency of extreme rainfall events will result in flooding that leads to damaged crops¹⁶ and
800 agricultural infrastructure that raises concerns about food security. Availability of water and
801 food will also influence livestock production²¹⁰.

802
803 Anthropogenic warming will also induce changes to large-scale biogeochemical cycles across
804 Eastern Africa, with the possibility to feedback on atmospheric GHG concentrations¹²⁷. Indeed,
805 the influence of rainfall variability on wetland methane emissions is expected to continue in
806 the future. For instance, CMIP5 simulations (Supplementary Information) predict methane
807 emissions will increase by $\sim 4\text{Tg yr}^{-1}$ under RCP4.5 and $\sim 11\text{Tg yr}^{-1}$ for RCP8.5 from 2000 to
808 2100 (Fig. 5a, b). These projected increases can be linked to increases in surface
809 temperature, inundation (via rainfall) and net primary production (also indirectly affected by
810 rainfall), each with similar importance (Fig. 5c). Moreover, future rainfall variability, namely the
811 projected increase in short rains, is expected to reduce the spatial extent of fires²¹¹ and
812 enhance above-ground biomass (and associated vegetation greening²¹² and increase in
813 NPP²¹³) with an accompanying transition to forest biomes over Eastern Africa^{214–216}. These
814 changes will each have subsequent effects on ecosystem functioning, carbon cycling and
815 broader biogeochemical storylines in the Earth System.

816
817 There is a threshold of relative humidity (and temperature) that limits the transmission of
818 malaria and arboviruses via their influence on the associated vectors (for example,
819 mosquitoes) and pathogens^{173,217,218}. Increases in relative humidity associated with more
820 extreme wet seasons in the future can shorten the incubation and blood-feeding stages²¹⁸ of
821 the mosquito life cycle, but the net impact of these changes is unclear. Increased future levels
822 of rainfall and its variability may also lead to more frequent and persistent flooding that will
823 help establish more breeding sites for insects, although some vectors breed indoors and will
824 be unaffected directly by flooding. The relationship between flooding and water-borne
825 diseases such as cholera and typhoid differs by region^{173,217}. However, one of the biggest risks
826 for future transmission of malaria and arboviruses in Eastern Africa is drug and insecticide
827 resistance combined with warmer temperatures and lower relative humidity associated with
828 climate change in the highland regions, where there is little immunity and insufficient health
829 infrastructure^{165,166,219,220}.

830 831 **6 Summary & future perspectives**

832
833 Eastern Africa suffers extreme seasonal and year-to-year variations in rainfall, driving
834 substantial environmental, social, and economic impacts. For instance, extreme changes in
835 hydroclimatic conditions during 2021, exacerbated by water management challenges, have
836 led to some of the worst flooding in South Sudan for the past sixty years, impacting food and
837 energy security, access to potable water, and the spread of waterborne disease and
838 arboviruses. Other parts of Eastern Africa, particularly countries in the Horn of Africa, are
839 experiencing prolonged and extensive drought due to consecutive La Niña events from 2020-
840 2022, exacerbated by GHG warming over the western Pacific. These droughts have resulted

841 in the collapse of agricultural crops and livestock that support subsistence farming across the
842 region.

843

844 While uncertain, there is some consensus that short rains totals (OND) will exceed those of
845 the long rains (MAM) in a warming climate, the timing of which is dependent on the scenario
846 but could occur as early as 2030. Regional climate models generally show a stronger rainfall
847 response to a warming climate, with models that resolve convection reporting even higher
848 extreme rainfall rates. This suggests that the vast majority of climate models, which still use
849 parametrised convection, are potentially underestimating future increases in rainfall and
850 therefore the subsequent impacts across Eastern Africa.

851

852 To minimize the risks associated with extreme variations in rainfall over Eastern Africa, several
853 priority areas of future research are required, all demanding the development of proactive
854 policies.

855

856 Improve meteorological observing networks and forecast systems

857 Improved early detection and weather forecast systems that focus on Eastern Africa will
858 engender better preparedness for extremes associated with seasonal changes in rainfall and
859 will inform decadal planning strategies. Development and evaluation of convective-permitting
860 regional climate models¹⁹¹ would provide further confidence in their ability to describe extreme
861 rainfall events that have disproportionately important impacts. Growing model skill in sub-
862 seasonal rainfall forecasts^{221–227} relies on improving model physics of the atmosphere and
863 ocean and on more and higher-quality data, particularly from satellites that include instruments
864 that observe atmosphere and ocean properties. Improved model simulations of the long rains
865 over Eastern Africa hinge on improving knowledge of the atmospheric state, particularly
866 humidity, over the Northwest Indian Ocean²²⁸, which could be tested with a dedicated
867 measurement campaign. Ocean interior measurements currently collected by arrays of buoys
868 across the tropics, particularly the Indian Ocean and western Pacific, could be expanded to
869 help reduce knowledge gaps²²⁹. To improve forecast skill of high-impact weather events over
870 Eastern Africa, targeted²³⁰ ground-based, airborne and shipborne observations could be
871 deployed to supplement existing operational data streams. Equally important are the
872 assimilation methods that optimise the use of these observations for improving model
873 simulations²³¹. Rescuing and sharing historical data over Africa would also improve climate
874 predictions²³².

875

876 Translating forecast analyses into actionable information is a key part of any system^{233,234}. The
877 Famine Early Warning Systems Network⁸³ is a good example of such a system. Delivering
878 useful information to countries requires detailed knowledge about national agricultural and
879 economic policies, evolving national political environments and the capability to communicate
880 with local farming communities and governments. Establishing long-term funding that supports
881 civilian data collecting, transcending lifecycles of individual governments, will help to provide
882 effective information about how to mitigate the worst climate impacts.

883

884 Improve environmental observing systems

885 Climate and weather forecast data can also help with disease forecasting¹⁶⁴ but this has not
886 been fully realised. Satellite observations of surface temperature, humidity and land use
887 change can be used to predict shifts in disease burden²³⁵ and hotspots for emerging zoonotic

diseases and how they will spread^{236–238}, and together with epidemiological data could form the basis of early detection systems over Eastern Africa¹⁶⁴.

Understanding quantitative changes in hydrology and the carbon cycle across Eastern Africa is currently limited to very few surface sites and broad inferences from satellite observations^{124,239}. Given the importance of water flows across the regions and subsequent impacts on water and food security and the carbon cycle there is a clear need for a more coordinated and sustainable measurement network to monitor variations²⁴⁰. More collaboration between African and international hydrologists, ecologists, and carbon cycle scientists will help facilitate this kind of activity.

Advance Earth System Models

Exploiting advances in observing systems and better understanding the carbon-water nexus must translate into commensurate improvements²³³ in physically based simulations of Eastern African climate, and how it relates to the broader climate system. A key recommendation is to develop a more robust understanding of the relationship between future levels of atmospheric GHG and changes in the frequency and variability of the IOD^{69,198,201,203,241,242}, and how future changes in ENSO and the IOD will influence rainfall over Eastern Africa¹⁸⁸ and in turn how that influences vegetation cover and subsequently the emission of methane¹²⁷. This point ties together the previous recommendations, and only by bringing together communities involved in measurements and model development can meaningful progress be made with identifying and prioritizing work on reducing uncertainty.

Improve freshwater security

Eastern Africa encompasses regions that are being flooded and regions that are subject to drought, both driven by large inter- and intra-seasonal changes in rainfall. In both extremes, there is an urgent need to improve national water storage infrastructure, flood protection and sanitation systems to improve the safety and security of freshwater resources to help increase agricultural output and a growing population²⁴³. This is a systemic challenge that requires co-development of water usage strategies between stakeholders and development agencies, informed by scenarios that account for changes in rainfall, land use, and the growing demands from an increase in population. Recommendations include investment in water-saving technologies and efficient management options such as the adoption of sprinkler and drip irrigation systems to replace commonly-used flood irrigation, and to invest in recycling wastewater when surface or groundwater reserves are insufficient²⁴³. Such an approach should also consider upstream and downstream water demands and losses, including the reduction of evaporative losses, particularly from catchment lakes and reservoirs in arid regions²⁴⁴ and the potential challenges and implications of adopting different approaches²⁴⁵.

Ensure food security

Ensuring future food security is related to the security of freshwater, with the agriculture sector generally having the lowest water use efficiency of all the water-using sectors²⁴⁶. How this sector will cope with changes in rainfall variability will depend on the nature of those changes. An upward trend in rainfall in some countries for different seasons, with an accompanying warming trend, may benefit some food crops that have a higher optimal growing temperature. However, if increased rainfall results from a higher frequency of extreme rainfall events that follow periods of drought, then flooding will become more of a challenge. Investment in better drainage systems is one solution, but in the longer term an increase in flooded areas that can

936 be managed may provide an opportunity to increase the use of floodplain agriculture, spate
937 irrigation²⁴⁷ or inundation canals. A shift in rainfall and surface water catchment areas may
938 result in a redistribution of crops being grown across Eastern Africa. Countries that will suffer
939 from more extensive droughts have other challenges to face. In this case, the agricultural
940 sector should invest in strategic rainwater and surface water storage options that provide
941 reliable flows but incur minimal additional losses, more efficient water management systems,
942 as described above, and distributing drought-tolerant seeds²⁴⁸ to maximize agricultural crop
943 yields during drought years. Widespread adoption of conservation tillage methods would
944 reduce water and soil loss, mainly by decreasing the intensity of the tillage and retention of
945 post-harvest plant residue²⁴⁹. Development of agricultural strategies to help farmers maximize
946 food production during good years would help mitigate impacts during drought years. Institutes
947 affiliated with the Consultative Group on International Agricultural Research continue to play
948 a key role in addressing those sustainable agricultural challenges.

949

950 All these recommendations require unprecedented levels of coordination and substantial
951 financial investment to link local to national scales, and in many cases will require trans-
952 boundary cooperation that will also involve extensive international diplomacy. Some activities
953 are underway, but some countries may require international financial aid to establish larger
954 activities that will eventually become self-sustaining. Without properly addressing the bigger
955 challenges now it becomes progressively more difficult for Eastern African countries to cope
956 with future variations in rainfall without incurring substantial humanitarian and economic
957 costs²⁵⁰ that will dwarf the multi-trillion dollar cost of the Covid-19 pandemic.

958

959 **Acknowledgements**

960 P.I.P., L.F., M.L. and R.P.A. acknowledge support from the UK National Centre for Earth
961 Observation (NCEO) funded by the National Environment Research Council (NE/R016518/1).
962 C.W. acknowledges funding of the Grantham Research Fellowship from the Grantham
963 Foundation. K.W. acknowledges Oxford Martin Programme on Transboundary Resource
964 Management. M.G. acknowledges the Coproduction of Climate Services for East Africa
965 project. B.D. and K.H. acknowledge support of the NCEO LTS-S and International Programme
966 (NE/X006328/1).

967

968 **Author contributions**

969 P.I.P. originated the review and coordinated the writing. P.I.P., C.M.W., B.D., R.I.M., K.G.W.,
970 N.G., J.E.H., N.M. and S.S.F. led the writing of individual subsections, with contributions from
971 R.P.A., C.M.W., B.D., R.I.M., N.G. and S.S.F. provided the figures. All authors helped to revise
972 and refine earlier drafts.

973

974 **Competing interests**

975 The authors declare no competing interests.

976

977 **References**

978

- 979 1. Gamoyo, M., Reason, C. & Obura, D. Rainfall variability over the East African coast.
980 *Theor. Appl. Climatol.* **120**, (2015).
- 981 2. Conway, D., Dalin, C., Landman, W. A. & Osborn, T. J. Hydropower plans in eastern
982 and southern Africa increase risk of concurrent climate-related electricity supply
983 disruption. *Nat. Energy* **2**, 946–953 (2017).

- 984 3. Ferrer, N. *et al.* Groundwater hydrodynamics of an Eastern Africa coastal aquifer,
985 including La Niña 2016–17 drought. *Sci. Total Environ.* **661**, (2019).
- 986 4. Adloff, M. *et al.* Sustained Water Storage in Horn of Africa Drylands Dominated by
987 Seasonal Rainfall Extremes. *Geophys. Res. Lett.* **49**, e2022GL099299 (2022).
- 988 5. Taylor, R. G. *et al.* Evidence of the dependence of groundwater resources on extreme
989 rainfall in East Africa. *Nat. Clim. Chang.* **3**, (2013).
- 990 6. Food Security and Nutrition Analysis Unit and Famine Early Warning System
991 Network. Somalia FSNAU Food Security & Nutrition Quarterly Brief - Focus on Post
992 Gu 2017 Season Early Warning. (2022).
- 993 7. World Bank Group. *Somalia drought impact and needs assessment : synthesis report.*
994 (2018).
- 995 8. Food Security and Nutrition Analysis Unit. Somalia faces Risk of Famine (IPC Phase
996 5) as multi-season drought and soaring food prices lead to worsening acute food
997 insecurity and malnutrition. <https://fsnau.org/node/1947> (2022).
- 998 9. UN Office for the Coordination of Humanitarian Affairs. *Horn of Africa Drought:*
999 *Regional Humanitarian Overview & Call to Action.* (2022).
- 1000 10. UN OCHA. *Humanitarian Needs Overview South Sudan. Humanitarian Programme*
1001 *Cycle 2021* (2021).
- 1002 11. Thomas, E. A. *et al.* Quantifying increased groundwater demand from prolonged
1003 drought in the East African Rift Valley. *Sci. Total Environ.* **666**, (2019).
- 1004 12. Elagib, N. A. *et al.* Debilitating floods in the Sahel are becoming frequent. *J. Hydrol.*
1005 **599**, 126362 (2021).
- 1006 13. Adhikari, U., Nejadhashemi, A. P. & Woznicki, S. A. Climate change and eastern
1007 Africa: a review of impact on major crops. *Food Energy Secur.* **4**, 110–132 (2015).
- 1008 14. Megersa, B. *et al.* Livestock Diversification: An Adaptive Strategy to Climate and
1009 Rangeland Ecosystem Changes in Southern Ethiopia. *Hum. Ecol.* **42**, (2014).
- 1010 15. Cook, K. H., Fitzpatrick, R. G. J., Liu, W. & Vizy, E. K. Seasonal asymmetry of
1011 equatorial East African rainfall projections: understanding differences between the
1012 response of the long rains and the short rains to increased greenhouse gases. *Clim.*
1013 *Dyn.* **55**, (2020).
- 1014 16. Wainwright, C. M., Finney, D. L., Kilavi, M., Black, E. & Marsham, J. H. Extreme
1015 Rainfall in East Africa October 2019 - January 2020 and context under Future Climate
1016 Change. *Weather (under Rev.)* (2020).
- 1017 17. Black, E., Slingo, J. & Sperber, K. R. An observational study of the relationship
1018 between excessively strong short rains in coastal East Africa and Indian ocean SST.
1019 *Mon. Weather Rev.* **131**, (2003).
- 1020 18. MacLeod, D., Graham, R., O'Reilly, C., Otieno, G. & Todd, M. Causal pathways
1021 linking different flavours of ENSO with the Greater Horn of Africa short rains. *Atmos.*
1022 *Sci. Lett.* **22**, (2021).
- 1023 19. Indeje, M., Semazzi, F. H. M. & Ogallo, L. J. ENSO signals in East African rainfall
1024 seasons. *Int. J. Climatol.* **20**, (2000).
- 1025 20. Wainwright, C. M., Marsham, J. H., Rowell, D. P., Finney, D. L. & Black, E. Future
1026 changes in seasonality in east africa from regional simulations with explicit and
1027 parameterized convection. *J. Clim.* **34**, (2021).
- 1028 21. Nicholson, S. E. Long-term variability of the East African 'short rains' and its links to
1029 large-scale factors. *Int. J. Climatol.* **35**, (2015).
- 1030 22. Jiang, Y., Zhou, L., Roundy, P. E., Hua, W. & Raghavendra, A. Increasing Influence of
1031 Indian Ocean Dipole on Precipitation Over Central Equatorial Africa. *Geophys. Res.*
1032 *Lett.* **48**, (2021).
- 1033 23. Funk, C. *et al.* Examining the role of unusually warm Indo-Pacific sea-surface
1034 temperatures in recent African droughts. *Q. J. R. Meteorol. Soc.* **144**, (2018).
- 1035 24. Shaaban, A. A. & Roundy, P. E. OLR perspective on the Indian Ocean Dipole with
1036 application to East African precipitation. *Q. J. R. Meteorol. Soc.* **143**, (2017).
- 1037 25. Zaitchik, B. F. Madden-Julian Oscillation impacts on tropical African precipitation.
1038 *Atmospheric Research* vol. 184 (2017).

- 1039 26. Pohl, B. & Camberlin, P. Influence of the Madden-Julian Oscillation on East African
1040 rainfall. II. March-May season extremes and interannual variability. *Q. J. R. Meteorol.*
1041 *Soc.* **132**, (2006).
- 1042 27. Pohl, B. & Camberlin, P. Influence of the Madden-Julian Oscillation on East African
1043 rainfall. I: Intraseasonal variability and regional dependency. *Q. J. R. Meteorol. Soc.*
1044 **132**, (2006).
- 1045 28. Finney, D. L. *et al.* The effect of westerlies on East African rainfall and the associated
1046 role of tropical cyclones and the Madden–Julian Oscillation. *Q. J. R. Meteorol. Soc.*
1047 **146**, (2020).
- 1048 29. Berhane, F. & Zaitchik, B. Modulation of daily precipitation over East Africa by the
1049 Madden-Julian oscillation. *J. Clim.* **27**, (2014).
- 1050 30. Vellinga, M. & Milton, S. F. Drivers of interannual variability of the East African “Long
1051 Rains”. *Q. J. R. Meteorol. Soc.* **144**, (2018).
- 1052 31. Martin, Z. *et al.* The influence of the quasi-biennial oscillation on the Madden–Julian
1053 oscillation. *Nature Reviews Earth and Environment* vol. 2 (2021).
- 1054 32. Gelaro, R. *et al.* The modern-era retrospective analysis for research and applications,
1055 version 2 (MERRA-2). *J. Clim.* **30**, 5419–5454 (2017).
- 1056 33. Huesmann, A. S. & Hitchman, M. H. The stratospheric quasi-biennial oscillation in the
1057 NCEP reanalyses: Climatological structures. *J. Geophys. Res. Atmos.* **106**, (2001).
- 1058 34. Indeje, M. & Semazzi, F. H. M. Relationships between QBO in the lower equatorial
1059 stratospheric zonal winds and East African seasonal rainfall. *Meteorol. Atmos. Phys.*
1060 **73**, (2000).
- 1061 35. Liu, W., Cook, K. H. & Vizzy, E. K. Influence of Indian Ocean SST regionality on the
1062 East African short rains. *Clim. Dyn.* **54**, (2020).
- 1063 36. Dyer, E. & Washington, R. Kenyan long rains: A subseasonal approach to process-
1064 based diagnostics. *J. Clim.* **34**, (2021).
- 1065 37. Kilavi, M. *et al.* Extreme Rainfall and Flooding over Central Kenya Including Nairobi
1066 City during the Long-Rains Season 2018: Causes, Predictability, and Potential for
1067 Early Warning and Actions. *Atmosphere (Basel)*. **9**, 472 (2018).
- 1068 38. Kebacho, L. L. The Role of Tropical Cyclones Idai and Kenneth in Modulating Rainfall
1069 Performance of 2019 Long Rains over East Africa. *Pure Appl. Geophys.* (2022)
1070 doi:10.1007/s00024-022-02993-2.
- 1071 39. Kebacho, L. L. Interannual variations of the monthly rainfall anomalies over Tanzania
1072 from March to May and their associated atmospheric circulations anomalies. *Nat.*
1073 *Hazards* (2022).
- 1074 40. Tarnavsky, E. *et al.* Extension of the TAMSAT satellite-based rainfall monitoring over
1075 Africa and from 1983 to present. *J. Appl. Meteorol. Climatol.* **53**, (2014).
- 1076 41. Maidment, R. I. *et al.* A new, long-term daily satellite-based rainfall dataset for
1077 operational monitoring in Africa. *Sci. Data* **4**, (2017).
- 1078 42. Dai, A. Hydroclimatic trends during 1950–2018 over global land. *Clim. Dyn.* **56**,
1079 (2021).
- 1080 43. Maidment, R. I., Allan, R. P. & Black, E. Recent observed and simulated changes in
1081 precipitation over Africa. *Geophys. Res. Lett.* **42**, (2015).
- 1082 44. Cattani, E., Merino, A., Guijarro, J. A. & Levizzani, V. East Africa Rainfall trends and
1083 variability 1983-2015 using three long-term satellite products. *Remote Sens.* **10**,
1084 (2018).
- 1085 45. Maidment, R. I. *et al.* The 30 year TAMSAT african rainfall climatology and time series
1086 (TARCAT) data set. *J. Geophys. Res.* **119**, (2014).
- 1087 46. Liebmann, B. *et al.* Climatology and interannual variability of boreal spring wet season
1088 precipitation in the eastern horn of Africa and implications for its recent decline. *J.*
1089 *Clim.* **30**, 3867–3886 (2017).
- 1090 47. Wainwright, C. M. *et al.* Eastern African Paradox rainfall decline due to shorter not
1091 less intense Long Rains. *npj Clim. Atmos. Sci.* **2**, (2019).
- 1092 48. Walker, D. P., Marsham, J. H., Birch, C. E., Scaife, A. A. & Finney, D. L. Common
1093 Mechanism for Interannual and Decadal Variability in the East African Long Rains.

- 1094 *Geophys. Res. Lett.* **47**, (2020).
- 1095 49. Nicholson, S. E. Climate and climatic variability of rainfall over eastern Africa. *Rev.*
1096 *Geophys.* **55**, (2017).
- 1097 50. Tierney, J. E., Ummenhofer, C. C. & deMenocal, P. B. Past and future rainfall in the
1098 Horn of Africa. *Sci. Adv.* **1**, e1500682 (2015).
- 1099 51. Saji, N. H., Goswami, B. N., Vinayachandran, P. N. & Yamagata, T. A dipole mode in
1100 the tropical Indian Ocean. *Nature* **401**, 360–363 (1999).
- 1101 52. Webster, P. J., Moore, A. M., Loschnigg, J. P. & Leben, R. R. Coupled ocean-
1102 atmosphere dynamics in the Indian Ocean during 1997-98. *Nature* **401**, (1999).
- 1103 53. Funk, C. *et al.* Examining the potential contributions of extreme 'western v' sea
1104 surface temperatures to the 2017 March-June east african drought. *Bull. Am.*
1105 *Meteorol. Soc.* **100**, (2019).
- 1106 54. Liebmann, B. *et al.* Climatology and interannual variability of boreal spring wet season
1107 precipitation in the eastern horn of Africa and implications for its recent decline. *J.*
1108 *Clim.* **30**, (2017).
- 1109 55. Thielke, A. & Mölg, T. Observed and simulated Indian Ocean Dipole activity since the
1110 mid-19th century and its relation to East African short rains. *Int. J. Climatol.* **39**,
1111 (2019).
- 1112 56. Trenberth, K. E., Fasullo, J. T., Branstator, G. & Phillips, A. S. Seasonal aspects of
1113 the recent pause in surface warming. *Nat. Clim. Chang.* **4**, (2014).
- 1114 57. L'Heureux, M. L., Lee, S. & Lyon, B. Recent multidecadal strengthening of the Walker
1115 circulation across the tropical Pacific. *Nat. Clim. Chang.* **3**, (2013).
- 1116 58. England, M. H. *et al.* Recent intensification of wind-driven circulation in the Pacific and
1117 the ongoing warming hiatus. *Nat. Clim. Chang.* **4**, (2014).
- 1118 59. Seager, R. *et al.* Strengthening tropical Pacific zonal sea surface temperature
1119 gradient consistent with rising greenhouse gases. *Nature Climate Change* vol. 9
1120 (2019).
- 1121 60. Black, E. The relationship between Indian Ocean sea-surface temperature and East
1122 African rainfall. *Philos. Trans. R. Soc. A Math. Phys. Eng. Sci.* **363**, (2005).
- 1123 61. Lyon, B. Seasonal drought in the Greater Horn of Africa and its recent increase during
1124 the March-May long rains. *J. Clim.* **27**, (2014).
- 1125 62. Allan, R. P. *et al.* Advances in understanding large-scale responses of the water cycle
1126 to climate change. *Annals of the New York Academy of Sciences* vol. 1472 (2020).
- 1127 63. Bronnimann, S. *et al.* Southward shift of the northern tropical belt from 1945 to 1980.
1128 *Nat. Geosci.* **8**, (2015).
- 1129 64. Undorf, S. *et al.* Detectable Impact of Local and Remote Anthropogenic Aerosols on
1130 the 20th Century Changes of West African and South Asian Monsoon Precipitation. *J.*
1131 *Geophys. Res. Atmos.* **123**, (2018).
- 1132 65. Dong, B. & Sutton, R. Dominant role of greenhouse-gas forcing in the recovery of
1133 Sahel rainfall. *Nat. Clim. Chang.* **5**, (2015).
- 1134 66. Blau, M. T. & Ha, K. J. The Indian Ocean Dipole and its Impact on East African Short
1135 Rains in Two CMIP5 Historical Scenarios With and Without Anthropogenic Influence.
1136 *J. Geophys. Res. Atmos.* **125**, (2020).
- 1137 67. Kew, S. F. *et al.* Impact of precipitation and increasing temperatures on drought
1138 trends in eastern Africa. *Earth Syst. Dyn.* **12**, (2021).
- 1139 68. Held, I. M. & Soden, B. J. Robust responses of the hydrological cycle to global
1140 warming. *J. Clim.* **19**, (2006).
- 1141 69. Vecchi, G. A. & Soden, B. J. Global warming and the weakening of the tropical
1142 circulation. *J. Clim.* **20**, (2007).
- 1143 70. Byrne, M. P. & Schneider, T. Narrowing of the ITCZ in a warming climate: Physical
1144 mechanisms. *Geophys. Res. Lett.* **43**, (2016).
- 1145 71. Byrne, M. P., Pendergrass, A. G., Rapp, A. D. & Wodzicki, K. R. Response of the
1146 Intertropical Convergence Zone to Climate Change: Location, Width, and Strength.
1147 *Current Climate Change Reports* vol. 4 (2018).
- 1148 72. Ayana, E. K., Ceccato, P., Fisher, J. R. B. & DeFries, R. Examining the relationship

- 1149 between environmental factors and conflict in pastoralist areas of East Africa. *Sci.*
 1150 *Total Environ.* **557–558**, (2016).
- 1151 73. Nakawuka, P., Langan, S., Schmitter, P. & Barron, J. A review of trends, constraints
 1152 and opportunities of smallholder irrigation in East Africa. *Glob. Food Sec.* **17**, 196–212
 1153 (2018).
- 1154 74. Alter, R. E., Im, E. S. & Eltahir, E. A. B. Rainfall consistently enhanced around the
 1155 Gezira Scheme in East Africa due to irrigation. *Nat. Geosci.* **8**, (2015).
- 1156 75. Vicente-Serrano, S. M. *et al.* Challenges for drought mitigation in Africa: The potential
 1157 use of geospatial data and drought information systems. *Appl. Geogr.* **34**, (2012).
- 1158 76. Mera, G. A. Drought and its impacts in Ethiopia. *Weather Clim. Extrem.* **22**, 24–35
 1159 (2018).
- 1160 77. Funk, C. Ethiopia, Somalia and Kenya face devastating drought. *Nature* **586**, 645
 1161 (2020).
- 1162 78. Korecha, D. & Barnston, A. G. Predictability of June–September rainfall in Ethiopia.
 1163 *Mon. Weather Rev.* **135**, (2007).
- 1164 79. Bachewe, F. N., Yimer, F., Minten, B. & Dorosh, P. A. *Agricultural prices during*
 1165 *drought in Ethiopia. ESSP Working Paper* vol. 97 (2016).
- 1166 80. Obasi, G. O. P. The impacts of ENSO in Africa. in *Climate Change and Africa* vol.
 1167 9780521836340 (2005).
- 1168 81. Desta, Z. H. & Oba, G. Feed scarcity and livestock mortality in enset farming systems
 1169 in the Bale highlands of southern Ethiopia. *Outlook Agric.* **33**, (2004).
- 1170 82. Habte, M., Eshetu, M., Maryo, M., Andualem, D. & Legesse, A. Effects of climate
 1171 variability on livestock productivity and pastoralists perception: The case of drought
 1172 resilience in Southeastern Ethiopia. *Vet. Anim. Sci.* **16**, (2022).
- 1173 83. Funk, C. *et al.* Recognizing the famine early warning systems network over 30 years
 1174 of drought early warning science advances and partnerships promoting global food
 1175 security. *Bull. Am. Meteorol. Soc.* **100**, (2019).
- 1176 84. Novella, N. S. & Thiaw, W. M. African rainfall climatology version 2 for famine early
 1177 warning systems. *J. Appl. Meteorol. Climatol.* **52**, 588–606 (2013).
- 1178 85. Backer, D. & Billing, T. Validating Famine Early Warning Systems Network projections
 1179 of food security in Africa, 2009–2020. *Glob. Food Sec.* **29**, (2021).
- 1180 86. Simtowe, F. *et al.* Heterogeneous seed access and information exposure: implications
 1181 for the adoption of drought-tolerant maize varieties in Uganda. *Agric. Food Econ.* **7**,
 1182 (2019).
- 1183 87. Philip, S. *et al.* The drought in Ethiopia, 2015. *Clim. Dev. Knowl. Netw. World Weather*
 1184 *Attrib. Initiat.* (2017).
- 1185 88. Toreti, A. *et al.* *Drought in East Africa August 2022.* (2022).
- 1186 89. Yang, M. *et al.* The role of climate in the trend and variability of Ethiopia’s cereal crop
 1187 yields. *Sci. Total Environ.* **723**, 137893 (2020).
- 1188 90. Wilkes, M. A. *et al.* Physical and biological controls on fine sediment transport and
 1189 storage in rivers. *Wiley Interdisciplinary Reviews: Water* vol. 6 (2019).
- 1190 91. Gebrehiwot, K. A. A review on waterlogging, salinization and drainage in Ethiopian
 1191 irrigated agriculture. *Sustain. Water Resour. Manag.* **4**, 55–62 (2018).
- 1192 92. Fenta, A. A. *et al.* Cropland expansion outweighs the monetary effect of declining
 1193 natural vegetation on ecosystem services in sub-Saharan Africa. *Ecosyst. Serv.* **45**,
 1194 101154 (2020).
- 1195 93. Showler, A. T. Locust 1 (Orthoptera: Acrididae) Outbreak in Africa and Asia, 1992–
 1196 1994: An Overview. *Am. Entomol.* (1995) doi:10.1093/ae/41.3.179.
- 1197 94. Foster, Z. J. The 1915 Locust Attack in Syria and Palestine and its Role in the Famine
 1198 During the First World War. *Middle East. Stud.* (2015)
 1199 doi:10.1080/00263206.2014.976624.
- 1200 95. Showler, A. T. & Potter, C. S. Synopsis of the 1986–1989 Desert Locust (Orthoptera:
 1201 Acrididae) Plague and the Concept of Strategic Control. *Am. Entomol.* **37**, (1991).
- 1202 96. Bennett, L. V. The development and termination of the 1968 plague of the desert
 1203 locust, *Schistocerca gregaria* (Forskål) (Orthoptera, Acrididae). *Bull. Entomol. Res.*

- 1204 **66**, (1976).
- 1205 97. Showler, A. T. & Lecoq, M. Incidence and ramifications of armed conflict in countries
1206 with major desert locust breeding areas. *Agronomy* (2021)
1207 doi:10.3390/AGRONOMY11010114.
- 1208 98. IPC. IPC Alert on Locusts by The Integrated Food Security Phase Classification.
1209 (2020).
- 1210 99. Kray, H. & Shetty, S. The locust plague: Fighting a crisis within a crisis. (2020).
- 1211 100. FAO. *Impact of Desert Locust Infestation on Household Livelihoods and Food*
1212 *Security in Ethiopia: Joint Assessment Findings*. (2020).
- 1213 101. Singh, V. K. & Roxy, M. K. A review of ocean-atmosphere interactions during tropical
1214 cyclones in the north Indian Ocean. *Earth-Science Reviews* vol. 226 (2022).
- 1215 102. Yuan, J. P. & Cao, J. North Indian Ocean tropical cyclone activities influenced by the
1216 Indian Ocean Dipole mode. *Sci. China Earth Sci.* **56**, (2013).
- 1217 103. Madani, N. *et al.* Below-surface water mediates the response of African forests to
1218 reduced rainfall. *Environ. Res. Lett.* **15**, (2020).
- 1219 104. Guan, K. *et al.* Photosynthetic seasonality of global tropical forests constrained by
1220 hydroclimate. *Nat. Geosci.* **8**, (2015).
- 1221 105. Madani, N., Kimball, J. S., Jones, L. A., Parazoo, N. C. & Guan, K. Global analysis of
1222 bioclimatic controls on ecosystem productivity using satellite observations of solar-
1223 induced chlorophyll fluorescence. *Remote Sens.* **9**, (2017).
- 1224 106. Schenk, H. J. & Jackson, R. B. Rooting depths, lateral root spreads and below-
1225 ground/above-ground allometries of plants in water-limited ecosystems. *J. Ecol.* **90**,
1226 (2002).
- 1227 107. Jones, L. A. *et al.* The SMAP Level 4 Carbon Product for Monitoring Ecosystem Land-
1228 Atmosphere CO₂ Exchange. *IEEE Trans. Geosci. Remote Sens.* **55**, (2017).
- 1229 108. Bauer, S. E., Im, U., Mezuman, K. & Gao, C. Y. Desert Dust, Industrialization, and
1230 Agricultural Fires: Health Impacts of Outdoor Air Pollution in Africa. *J. Geophys. Res.*
1231 *Atmos.* **124**, (2019).
- 1232 109. Jaeglé, L., Steinberger, L., Martin, R. V. & Chance, K. Global partitioning of NO_x
1233 sources using satellite observations: Relative roles of fossil fuel combustion, biomass
1234 burning and soil emissions. in *Faraday Discussions* vol. 130 (2005).
- 1235 110. van der Werf, G. R. *et al.* Global fire emissions estimates during 1997--2016. *Earth*
1236 *Syst. Sci. Data* **9**, 697–720 (2017).
- 1237 111. Bistinas, I., Harrison, S. P., Prentice, I. C. & Pereira, J. M. C. Causal relationships
1238 versus emergent patterns in the global controls of fire frequency. *Biogeosciences* **11**,
1239 (2014).
- 1240 112. Finney, D. L. *et al.* African Lightning and its Relation to Rainfall and Climate Change
1241 in a Convection-Permitting Model. *Geophys. Res. Lett.* **47**, (2020).
- 1242 113. Andela, N. *et al.* A human-driven decline in global burned area. *Science* (80-.). **356**,
1243 (2017).
- 1244 114. Andela, N. & Van Der Werf, G. R. Recent trends in African fires driven by cropland
1245 expansion and El Niño to la Niña transition. *Nat. Clim. Chang.* **4**, (2014).
- 1246 115. Chen, Y. *et al.* A pan-tropical cascade of fire driven by El Niño/Southern Oscillation.
1247 *Nat. Clim. Chang.* **7**, (2017).
- 1248 116. Kim, I. W. *et al.* Tropical Indo-Pacific SST influences on vegetation variability in
1249 eastern Africa. *Sci. Rep.* **11**, (2021).
- 1250 117. Ringeval, B. *et al.* An attempt to quantify the impact of changes in wetland extent on
1251 methane emissions on the seasonal and interannual time scales. *Global Biogeochem.*
1252 *Cycles* (2010) doi:10.1029/2008GB003354.
- 1253 118. Bloom, A. A., Palmer, P. I., Fraser, A., David, S. R. & Frankenberg, C. Large-scale
1254 controls of methanogenesis inferred from methane and gravity spaceborne data.
1255 *Science* (80-.). (2010) doi:10.1126/science.1175176.
- 1256 119. Whalen, S. C. Biogeochemistry of methane exchange between natural wetlands and
1257 the atmosphere. *Environmental Engineering Science* (2005)
1258 doi:10.1089/ees.2005.22.73.

- 1259 120. Bloom, A. A., Palmer, P. I., Fraser, A., Reay, D. S. & Frankenberg, C. Large-Scale
1260 Controls of Methanogenesis Inferred from Methane and Gravity Spaceborne Data.
1261 *Science* (80-.). **327**, 322–325 (2010).
- 1262 121. Helfter, C. *et al.* Phenology is the dominant control of methane emissions in a tropical
1263 non-forested wetland. *Nat. Commun.* **13**, 133 (2022).
- 1264 122. Joabsson, A., Christensen, T. R. & Wallén, B. Vascular plant controls on methane
1265 emissions from northern peatforming wetlands. *Trends in Ecology and Evolution*
1266 (1999) doi:10.1016/S0169-5347(99)01649-3.
- 1267 123. Dingemans, B. J. J., Barker, E. S. & Bodelier, P. L. E. Aquatic herbivores facilitate the
1268 emission of methane from wetlands. *Ecology* (2011) doi:10.1890/10-1297.1.
- 1269 124. Lunt, M. F. *et al.* An increase in methane emissions from tropical Africa between 2010
1270 and 2016 inferred from satellite data. *Atmos. Chem. Phys.* **19**, 14721–14740 (2019).
- 1271 125. Lunt, M. F. *et al.* Rain-fed pulses of methane from East Africa during 2018-2019
1272 contributed to atmospheric growth rate. *Environ. Res. Lett.* **16**, 24021 (2021).
- 1273 126. Pandey, S. *et al.* Using satellite data to identify the methane emission controls of
1274 South Sudan's wetlands. *Biogeosciences* (2021) doi:10.5194/bg-18-557-2021.
- 1275 127. Feng, L., Palmer, P. I., Zhu, S., Parker, R. J. & Liu, Y. Tropical methane emissions
1276 explain large fraction of recent changes in global atmospheric methane growth rate.
1277 *Nat. Commun.* **13**, 1378 (2022).
- 1278 128. Sutcliffe, J. V. & Parks, Y. P. *The hydrology of the Nile. The hydrology of the Nile.*
1279 *IAHS Special Publication No.5.* (1999).
- 1280 129. Sutcliffe, J. & Brown, E. Water losses from the Sudd. *Hydrol. Sci. J.* (2018)
1281 doi:10.1080/02626667.2018.1438612.
- 1282 130. Lunt, M. F. *et al.* Rain-fed pulses of methane from East Africa during 2018-2019
1283 contributed to atmospheric growth rate. *Environ. Res. Lett.* **16**, 24021 (2021).
- 1284 131. Qu, Z. *et al.* Attribution of the 2020 surge in atmospheric methane by inverse analysis
1285 of GOSAT observations. *Environ. Res. Lett.* **17**, 094003 (2022).
- 1286 132. Feng, L., Palmer, P. I., Parker, R. J., Lunt, M. F. & Boesch, H. Methane emissions
1287 responsible for record-breaking atmospheric methane growth rates in 2020 and 2021.
1288 *Atmos. Chem. Phys. Discuss.* **2022**, 1–23 (2022).
- 1289 133. Van Damme, M. *et al.* Industrial and agricultural ammonia point sources exposed.
1290 *Nature* **564**, (2018).
- 1291 134. Dammers, E. *et al.* NH₃ emissions from large point sources derived from CrIS and
1292 IASI satellite observations. *Atmos. Chem. Phys.* **19**, (2019).
- 1293 135. Bauer, S. E., Tsigaridis, K. & Miller, R. Significant atmospheric aerosol pollution
1294 caused by world food cultivation. *Geophys. Res. Lett.* **43**, (2016).
- 1295 136. Lelieveld, J., Evans, J. S., Fnais, M., Giannadaki, D. & Pozzer, A. The contribution of
1296 outdoor air pollution sources to premature mortality on a global scale. *Nature* **525**,
1297 (2015).
- 1298 137. Denier Van Der Gon, H. & Bleeker, A. Indirect N₂O emission due to atmospheric N
1299 deposition for the Netherlands. *Atmos. Environ.* **39**, (2005).
- 1300 138. Krupa, S. V. Effects of atmospheric ammonia (NH₃) on terrestrial vegetation: A
1301 review. *Environmental Pollution* vol. 124 (2003).
- 1302 139. Matson, P. A., McDowell, W. H., Townsend, A. R. & Vitousek, P. M. The globalization
1303 of N deposition: Ecosystem consequences in tropical environments. *Biogeochemistry*
1304 **46**, (1999).
- 1305 140. Tian, D. & Niu, S. A global analysis of soil acidification caused by nitrogen addition.
1306 *Environ. Res. Lett.* **10**, (2015).
- 1307 141. Koutsoyiannis, D., Yao, H. & Georgakakos, A. Medium-range flow prediction for the
1308 Nile: a comparison of stochastic and deterministic methods / Prévision du débit du Nil
1309 à moyen terme: une comparaison de méthodes stochastiques et déterministes.
1310 *Hydrol. Sci. J.* **53**, 142–164 (2008).
- 1311 142. Kim, M. & Or, D. Microscale pH variations during drying of soils and desert biocrusts
1312 affect HONO and NH₃ emissions. *Nat. Commun.* **10**, (2019).
- 1313 143. Roelle, P. A. & Aneja, V. P. Characterization of ammonia emissions from soils in the

- 1314 upper coastal plain, North Carolina. *Atmos. Environ.* **36**, (2002).
- 1315 144. Clarisse, L. *et al.* Atmospheric ammonia (NH₃) emanations from Lake Natron's
1316 saline mudflats. *Sci. Rep.* **9**, (2019).
- 1317 145. Hickman, J. E. *et al.* Changes in biomass burning, wetland extent, or agriculture drive
1318 atmospheric NH₃ trends in select African regions. *Atmos. Chem. Phys.* **21**, (2021).
- 1319 146. Di Vittorio, C. A. & Georgakakos, A. P. Land cover classification and wetland
1320 inundation mapping using MODIS. *Remote Sens. Environ.* **204**, (2018).
- 1321 147. Oluwasanya, G. . P. D. . Q. M. . S. V. *Water Security in Africa: A Preliminary*
1322 *Assessment* . (2022).
- 1323 148. Sridharan, V. *et al.* Resilience of the Eastern African electricity sector to climate driven
1324 changes in hydropower generation. *Nat. Commun.* **10**, 302 (2019).
- 1325 149. Jeuland, M. Economic implications of climate change for infrastructure planning in
1326 transboundary water systems: An example from the Blue Nile. *Water Resour. Res.*
1327 **46**, W11556 (2010).
- 1328 150. Jeuland, M. & Whittington, D. Water resources planning under climate change:
1329 Assessing the robustness of real options for the Blue Nile. *Water Resour. Res.* **50**,
1330 2086–2107 (2014).
- 1331 151. Conway, D. Water resources: Future Nile river flows. *Nat. Clim. Chang.* **7**, 319–320
1332 (2017).
- 1333 152. Siderius, C. *et al.* Hydrological Response and Complex Impact Pathways of the
1334 2015/2016 El Niño in Eastern and Southern Africa. *Earth's Futur.* **6**, (2018).
- 1335 153. Samboko, P. *et al.* The Impact of Power Rationing on Zambia's Agricultural Sector.
1336 *Work. Pap. No. 105* (2016).
- 1337 154. Dinar, A., Blankespoor, B., Dinar, S. & Kurukulasuriya, P. Does precipitation and
1338 runoff variability affect treaty cooperation between states sharing international bilateral
1339 rivers? *Ecol. Econ.* **69**, 2568–2581 (2010).
- 1340 155. Wheeler, K. G., Jeuland, M., Hall, J. W., Zagana, E. & Whittington, D. Understanding
1341 and managing new risks on the Nile with the Grand Ethiopian Renaissance Dam. *Nat.*
1342 *Commun.* **11**, 5222 (2020).
- 1343 156. Peña-Ramos, J. A., José López-Bedmar, R., Sastre, F. J. & Martínez-Martínez, A.
1344 Water Conflicts in Sub-Saharan Africa. *Front. Environ. Sci.* **10**, (2022).
- 1345 157. Wolf, A. T. Shared Waters: Conflict and Cooperation. *Annu. Rev. Environ. Resour.* **32**,
1346 241–269 (2007).
- 1347 158. Wheeler, K. G. *et al.* Cooperative filling approaches for the Grand Ethiopian
1348 Renaissance Dam. *Water Int.* **41**, 611–634 (2016).
- 1349 159. Calderón, C. & Servén, L. Infrastructure and Economic Development in Sub-Saharan
1350 Africa †. *J. Afr. Econ.* **19**, i13–i87 (2010).
- 1351 160. Douglas, I. *et al.* Unjust waters: climate change, flooding and the urban poor in Africa.
1352 *Environ. Urban.* **20**, 187–205 (2008).
- 1353 161. Birhanu, D., Kim, H., Jang, C. & Park, S. Flood Risk and Vulnerability of Addis Ababa
1354 City Due to Climate Change and Urbanization. *Procedia Eng.* **154**, 696–702 (2016).
- 1355 162. Mahmood, M. I., Elagib, N. A., Horn, F. & Saad, S. A. G. Lessons learned from
1356 Khartoum flash flood impacts: An integrated assessment. *Sci. Total Environ.* **601–**
1357 **602**, 1031–1045 (2017).
- 1358 163. AFB. Flooding: Sudan. *Africa Res. Bull. Econ. Financ. Tech. Ser.* **57**, 23103A-23106C
1359 (2020).
- 1360 164. Thomson, M. C., Muñoz, Á. G., Cousin, R. & Shumake-Guillemot, J. Climate drivers
1361 of vector-borne diseases in Africa and their relevance to control programmes. *Infect.*
1362 *Dis. Poverty* (2018) doi:10.1186/s40249-018-0460-1.
- 1363 165. Caminade, C., McIntyre, K. M. & Jones, A. E. Impact of recent and future climate
1364 change on vector-borne diseases. *Annals of the New York Academy of Sciences*
1365 (2019) doi:10.1111/nyas.13950.
- 1366 166. Endo, N. & Eltahir, E. A. B. Increased risk of malaria transmission with warming
1367 temperature in the Ethiopian Highlands. *Environ. Res. Lett.* **15**, 54006 (2020).
- 1368 167. Brown, V., Issak, M. A., Rossi, M., Barboza, P. & Paugam, A. Epidemic of malaria in

- 1369 north-eastern Kenya. *Lancet* (1998) doi:10.1016/S0140-6736(05)60747-7.
- 1370 168. Kilian, A. H. D., Langi, P., Talisuna, A. & Kabagambe, G. Rainfall pattern, El Nino and
1371 malaria in Uganda. *Trans. R. Soc. Trop. Med. Hyg.* (1999) doi:10.1016/S0035-
1372 9203(99)90165-7.
- 1373 169. Boyce, R. *et al.* Severe Flooding and Malaria Transmission in the Western Ugandan
1374 Highlands: Implications for Disease Control in an Era of Global Climate Change. *J.*
1375 *Infect. Dis.* (2016) doi:10.1093/infdis/jiw363.
- 1376 170. Nosrat, C. *et al.* Impact of recent climate extremes on mosquito-borne disease
1377 transmission in kenya. *PLoS Negl. Trop. Dis.* (2021)
1378 doi:10.1371/journal.pntd.0009182.
- 1379 171. Hashizume, M., Terao, T. & Minakawa, N. The Indian Ocean Dipole and malaria risk
1380 in the highlands of western Kenya. *Proc. Natl. Acad. Sci. U. S. A.* (2009)
1381 doi:10.1073/pnas.0806544106.
- 1382 172. Hashizume, M., Chaves, L. F. & Minakawa, N. Indian Ocean Dipole drives malaria
1383 resurgence in East African highlands. *Sci. Rep.* (2012) doi:10.1038/srep00269.
- 1384 173. Moore, S. M. *et al.* El Niño and the shifting geography of cholera in Africa. *Proc. Natl.*
1385 *Acad. Sci. U. S. A.* (2017) doi:10.1073/pnas.1617218114.
- 1386 174. Rieckmann, A., Tamason, C. C., Gurley, E. S., Rod, N. H. & Jensen, P. K. M.
1387 Exploring droughts and floods and their association with cholera outbreaks in sub-
1388 saharan africa: a register-based ecological study from 1990 to 2010. *Am. J. Trop.*
1389 *Med. Hyg.* (2018) doi:10.4269/ajtmh.17-0778.
- 1390 175. Lindsay, S. W., Bødker, R., Malima, R., Msangeni, H. A. & Kisinza, W. Effect of 1997-
1391 98 El Nino on highland malaria in Tanzania. *Lancet* (2000) doi:10.1016/S0140-
1392 6736(00)90022-9.
- 1393 176. Chemura, A., Mudereri, B. T., Yalew, A. W. & Gornott, C. Climate change and
1394 specialty coffee potential in Ethiopia. *Sci. Rep.* **11**, (2021).
- 1395 177. Lobell, D. B. & Burke, M. B. Why are agricultural impacts of climate change so
1396 uncertain? the importance of temperature relative to precipitation. *Environ. Res. Lett.*
1397 **3**, (2008).
- 1398 178. Tigchelaar, M., Battisti, D. S., Naylor, R. L. & Ray, D. K. Future warming increases
1399 probability of globally synchronized maize production shocks. *Proc. Natl. Acad. Sci. U.*
1400 *S. A.* **115**, (2018).
- 1401 179. Shapiro, L. L. M., Whitehead, S. A. & Thomas, M. B. Quantifying the effects of
1402 temperature on mosquito and parasite traits that determine the transmission potential
1403 of human malaria. *PLoS Biol.* **15**, (2017).
- 1404 180. Yang, W., Seager, R., Cane, M. A. & Lyon, B. The East African long rains in
1405 observations and models. *J. Clim.* **27**, (2014).
- 1406 181. Rowell, D. P., Booth, B. B. B., Nicholson, S. E. & Good, P. Reconciling past and
1407 future rainfall trends over East Africa. *J. Clim.* **28**, (2015).
- 1408 182. Dunning, C. M., Black, E. & Allan, R. P. Later Wet Seasons with More Intense Rainfall
1409 over Africa under Future Climate Change. *J. Clim.* **31**, 9719–9738 (2018).
- 1410 183. Makula, E. K. & Zhou, B. Coupled Model Intercomparison Project phase 6 evaluation
1411 and projection of East African precipitation. *Int. J. Climatol.* (2021)
1412 doi:10.1002/joc.7373.
- 1413 184. Cook, B. I. *et al.* Twenty-First Century Drought Projections in the CMIP6 Forcing
1414 Scenarios. *Earth's Futur.* **8**, (2020).
- 1415 185. Ongoma, V., Chena, H. & Gaoa, C. Projected changes in mean rainfall and
1416 temperature over east Africa based on CMIP5 models. *Int. J. Climatol.* **38**, (2018).
- 1417 186. Akinsanola, A. A., Ongoma, V. & Kooperman, G. J. Evaluation of CMIP6 models in
1418 simulating the statistics of extreme precipitation over Eastern Africa. *Atmos. Res.* **254**,
1419 (2021).
- 1420 187. Rowell, D. P., Senior, C. A., Vellinga, M. & Graham, R. J. Can climate projection
1421 uncertainty be constrained over Africa using metrics of contemporary performance?
1422 *Clim. Change* **134**, (2016).
- 1423 188. Endris, H. S. *et al.* Future changes in rainfall associated with ENSO, IOD and

- 1424 changes in the mean state over Eastern Africa. *Clim. Dyn.* **52**, (2019).
- 1425 189. Ayugi, B. *et al.* Comparison of CMIP6 and CMIP5 models in simulating mean and
1426 extreme precipitation over East Africa. *Int. J. Climatol.* **41**, (2021).
- 1427 190. Iturbide, M. *et al.* Repository supporting the implementation of FAIR principles in the
1428 IPCC-WG1 Atlas. (2021) doi:10.5281/zenodo.3691645.
- 1429 191. Finney, D. L. *et al.* Effects of Explicit Convection on Future Projections of Mesoscale
1430 Circulations, Rainfall, and Rainfall Extremes over Eastern Africa. *J. Clim.* **33**, 2701–
1431 2718 (2020).
- 1432 192. Lyon, B. Biases in sea surface temperature and the annual cycle of Greater Horn of
1433 Africa rainfall in CMIP6. *Int. J. Climatol.* (2021) doi:10.1002/joc.7456.
- 1434 193. King, J. A., Washington, R. & Engelstaedter, S. Representation of the Indian Ocean
1435 Walker circulation in climate models and links to Kenyan rainfall. *Int. J. Climatol.* **41**,
1436 (2021).
- 1437 194. Cai, W. *et al.* Changing El Niño–Southern Oscillation in a warming climate. *Nature*
1438 *Reviews Earth and Environment* vol. 2 (2021).
- 1439 195. Zelle, H., van Oldenborgh, G. J., Burgers, G. & Dijkstra, H. El Niño and greenhouse
1440 warming: Results from ensemble simulations with the NCAR CCSM. *J. Clim.* **18**,
1441 (2005).
- 1442 196. Merryfield, W. J. Changes to ENSO under CO₂ doubling in a multimodel ensemble. *J.*
1443 *Clim.* **19**, (2006).
- 1444 197. Collins, M. *et al.* The impact of global warming on the tropical Pacific Ocean and El
1445 Niño. *Nat. Geosci.* **3**, (2010).
- 1446 198. Cai, W. *et al.* Increasing frequency of extreme El Niño events due to greenhouse
1447 warming. *Nat. Clim. Chang.* **4**, (2014).
- 1448 199. Cai, W. *et al.* ENSO and greenhouse warming. *Nature Climate Change* vol. 5 (2015).
- 1449 200. Singh, J. *et al.* Enhanced risk of concurrent regional droughts with increased ENSO
1450 variability and warming. *Nat. Clim. Chang.* **12**, 163–170 (2022).
- 1451 201. Zheng, X. T. *et al.* Indian ocean dipole response to global warming in the CMIP5
1452 multimodel ensemble. *J. Clim.* **26**, (2013).
- 1453 202. Cai, W. & Cowan, T. Why is the amplitude of the Indian ocean dipole overly large in
1454 CMIP3 and CMIP5 climate models? *Geophys. Res. Lett.* **40**, (2013).
- 1455 203. Cai, W. *et al.* Opposite response of strong and moderate positive Indian Ocean Dipole
1456 to global warming. *Nat. Clim. Chang.* **11**, (2021).
- 1457 204. Douville, H. *et al.* Climate Change 2021: The Physical Science Basis. Contribution of
1458 Working Group I to the Sixth Assessment Report of the Intergovernmental Panel on
1459 Climate Change. in (Cambridge University Press, 2021).
- 1460 205. Chu, J. E. *et al.* Future change of the Indian Ocean basin-wide and dipole modes in
1461 the CMIP5. *Clim. Dyn.* **43**, (2014).
- 1462 206. Mamalakis, A. *et al.* Zonally contrasting shifts of the tropical rain belt in response to
1463 climate change. *Nat. Clim. Chang.* **11**, (2021).
- 1464 207. Schlenker, W. & Roberts, M. J. Nonlinear temperature effects indicate severe
1465 damages to U.S. crop yields under climate change. *Proc. Natl. Acad. Sci. U. S. A.*
1466 **106**, (2009).
- 1467 208. Wang, X., Xie, H., Guan, H. & Zhou, X. Different responses of MODIS-derived NDVI
1468 to root-zone soil moisture in semi-arid and humid regions. *J. Hydrol.* **340**, (2007).
- 1469 209. Guido, Z. *et al.* Farmer forecasts: Impacts of seasonal rainfall expectations on
1470 agricultural decision-making in Sub-Saharan Africa. *Clim. Risk Manag.* **30**, (2020).
- 1471 210. Thornton, P. K., van de Steeg, J., Notenbaert, A. & Herrero, M. The impacts of climate
1472 change on livestock and livestock systems in developing countries: A review of what
1473 we know and what we need to know. *Agricultural Systems* vol. 101 (2009).
- 1474 211. Senande-Rivera, M., Insua-Costa, D. & Miguez-Macho, G. Spatial and temporal
1475 expansion of global wildland fire activity in response to climate change. *Nat. Commun.*
1476 **13**, 1208 (2022).
- 1477 212. Piao, S. *et al.* Characteristics, drivers and feedbacks of global greening. *Nature*
1478 *Reviews Earth and Environment* vol. 1 (2020).

- 1479 213. Zarei, A., Chemura, A., Gleixner, S. & Hoff, H. Evaluating the grassland NPP
1480 dynamics in response to climate change in Tanzania. *Ecol. Indic.* **125**, (2021).
- 1481 214. Martens, C. *et al.* Large uncertainties in future biome changes in Africa call for flexible
1482 climate adaptation strategies. *Glob. Chang. Biol.* **27**, (2021).
- 1483 215. Doherty, R. M., Sitch, S., Smith, B., Lewis, S. L. & Thornton, P. K. Implications of
1484 future climate and atmospheric CO₂ content for regional biogeochemistry,
1485 biogeography and ecosystem services across East Africa. *Glob. Chang. Biol.* **16**,
1486 (2010).
- 1487 216. Scheiter, S. & Higgins, S. I. Impacts of climate change on the vegetation of Africa: An
1488 adaptive dynamic vegetation modelling approach. *Glob. Chang. Biol.* **15**, (2009).
- 1489 217. Kim, J. H. *et al.* A Systematic Review of Typhoid Fever Occurrence in Africa. *Clinical*
1490 *Infectious Diseases* vol. 69 (2019).
- 1491 218. Lahondre, C. & Lazzari, C. R. Mosquitoes cool down during blood feeding to avoid
1492 overheating. *Curr. Biol.* **22**, (2012).
- 1493 219. Colón-González, F. J. *et al.* Projecting the risk of mosquito-borne diseases in a
1494 warmer and more populated world: a multi-model, multi-scenario intercomparison
1495 modelling study. *Lancet Planet. Heal.* **5**, (2021).
- 1496 220. Ryan, S. J., Lippi, C. A. & Zermoglio, F. Shifting transmission risk for malaria in Africa
1497 with climate change: A framework for planning and intervention. *Malar. J.* **19**, (2020).
- 1498 221. Kolstad, E. W., MacLeod, D. & Demissie, T. D. Drivers of Subseasonal Forecast
1499 Errors of the East African Short Rains. *Geophys. Res. Lett.* **48**, (2021).
- 1500 222. Ogutu, G. E. O., Franssen, W. H. P., Supit, I., Omondi, P. & Hutjes, R. W. A. Skill of
1501 ECMWF system-4 ensemble seasonal climate forecasts for East Africa. *Int. J.*
1502 *Climatol.* **37**, (2017).
- 1503 223. Young, H. R. & Klingaman, N. P. Skill of seasonal rainfall and temperature forecasts
1504 for East Africa. *Weather Forecast.* **35**, (2020).
- 1505 224. Funk, C. *et al.* Predicting East African spring droughts using Pacific and Indian Ocean
1506 sea surface temperature indices. *Hydrol. Earth Syst. Sci.* **18**, (2014).
- 1507 225. Mutai, C. C., Ward, M. N. & Colman, A. W. Towards the prediction of the East Africa
1508 short rains based on sea-surface temperature-atmosphere coupling. *Int. J. Climatol.*
1509 **18**, (1998).
- 1510 226. Nicholson, S. E. The predictability of rainfall over the greater horn of Africa. Part I:
1511 Prediction of seasonal rainfall. *J. Hydrometeorol.* **15**, (2014).
- 1512 227. Meehl, G. A. *et al.* Initialized Earth System prediction from subseasonal to decadal
1513 timescales. *Nature Reviews Earth and Environment* vol. 2 (2021).
- 1514 228. MacLeod, D. Seasonal forecasts of the East African long rains: insight from
1515 atmospheric relaxation experiments. *Clim. Dyn.* **53**, (2019).
- 1516 229. Phillips, H. E. *et al.* Progress in understanding of Indian Ocean circulation, variability,
1517 air-sea exchange, and impacts on biogeochemistry. *Ocean Science* vol. 17 (2021).
- 1518 230. Majumdar, S. J. A review of targeted observations. *Bulletin of the American*
1519 *Meteorological Society* vol. 97 (2016).
- 1520 231. Dong, B., Haines, K. & Martin, M. Improved High Resolution Ocean Reanalyses Using
1521 a Simple Smoother Algorithm. *J. Adv. Model. Earth Syst.* **13**, (2021).
- 1522 232. Nordling, L. Scientists struggle to access Africa's historical climate data. *Nature* vol.
1523 574 (2019).
- 1524 233. Smith, M. J. *et al.* Changing how earth system modeling is done to provide more
1525 useful information for decision making, science, and society. *Bulletin of the American*
1526 *Meteorological Society* vol. 95 (2014).
- 1527 234. Webster, P. J. Meteorology: Improve weather forecasts for the developing world.
1528 *Nature* vol. 493 (2013).
- 1529 235. Mordecai, E. A., Ryan, S. J., Caldwell, J. M., Shah, M. M. & LaBeaud, A. D. Climate
1530 change could shift disease burden from malaria to arboviruses in Africa. *Lancet*
1531 *Planet. Heal.* **4**, e416–e423 (2020).
- 1532 236. Allen, T. *et al.* Global hotspots and correlates of emerging zoonotic diseases. *Nat.*
1533 *Commun.* **8**, (2017).

- 1534 237. Lipp, E. K., Huq, A. & Colwell, R. R. Effects of global climate on infectious disease:
1535 The cholera model. *Clinical Microbiology Reviews* vol. 15 (2002).
- 1536 238. Tamerius, J. D. *et al.* Environmental Predictors of Seasonal Influenza Epidemics
1537 across Temperate and Tropical Climates. *PLoS Pathog.* **9**, (2013).
- 1538 239. Palmer, P. I. *et al.* Net carbon emissions from African biosphere dominate pan-tropical
1539 atmospheric CO₂ signal. *Nat. Commun.* **10**, 3344 (2019).
- 1540 240. Merbold, L. *et al.* Opportunities for an African greenhouse gas observation system.
1541 *Reg. Environ. Chang.* **21**, (2021).
- 1542 241. Wang, T. *et al.* Why is the Indo-Gangetic Plain the region with the largest NH 3
1543 column in the globe during pre-monsoon and monsoon seasons? *Atmos. Chem.*
1544 *Phys.* **20**, 8727–8736 (2020).
- 1545 242. Cai, W. *et al.* Projected response of the Indian Ocean Dipole to greenhouse warming.
1546 *Nature Geoscience* vol. 6 (2013).
- 1547 243. Tramberend, S. *et al.* Co-development of East African regional water scenarios for
1548 2050. *One Earth* **4**, (2021).
- 1549 244. Zhao, G., Li, Y., Zhou, L. & Gao, H. Evaporative water loss of 1.42 million global
1550 lakes. *Nat. Commun.* **13**, 3686 (2022).
- 1551 245. Haghghi, E., Madani, K. & Hoekstra, A. Y. The water footprint of water conservation
1552 using shade balls in California. *Nat. Sustain.* **1**, (2018).
- 1553 246. FAO and UN Water. *Progress on change in water-use efficiency. Global status and*
1554 *acceleration needs for SDG indicator 6.4.1.* (2021).
- 1555 247. Acreman, M. C. *et al.* Managed flood releases from reservoirs: issues and guidance.
1556 *Rep. to DFID World Comm. Dams. Cent. Ecol. Hydrol. Wallingford, UK 2000*, p86
1557 (2000).
- 1558 248. Wang, J. *et al.* Exploitation of drought tolerance-related genes for crop improvement.
1559 *International Journal of Molecular Sciences* vol. 22 (2021).
- 1560 249. Biamah, E. K., Gichuki, F. N. & Kaumbutho, P. G. Tillage methods and soil and water
1561 conservation in eastern Africa. *Soil Tillage Res.* **27**, (1993).
- 1562 250. Parncutt, R. The human cost of anthropogenic global warming: Semi-quantitative
1563 prediction and the 1,000-tonne rule. *Front. Psychol.* **10**, (2019).
- 1564 251. Schreck, C. J. & Semazzi, F. H. M. Variability of the recent climate of eastern Africa.
1565 *Int. J. Climatol.* **24**, 681–701 (2004).
- 1566 252. Sutcliffe, J. & Parks, Y. *The hydrology of the Nile.* (IAHS Press, 1999).
- 1567 253. Alsdorf, D. *et al.* Opportunities for hydrologic research in the Congo Basin. *Reviews of*
1568 *Geophysics* vol. 54 (2016).
- 1569 254. Lehner, B. & Grill, G. Global river hydrography and network routing: Baseline data and
1570 new approaches to study the world's large river systems. *Hydrol. Process.* **27**, (2013).
- 1571 255. Becker, A. *et al.* A description of the global land-surface precipitation data products of
1572 the Global Precipitation Climatology Centre with sample applications including
1573 centennial (trend) analysis from 1901-present. *Earth Syst. Sci. Data* **5**, (2013).
- 1574 256. Schneider, U. *et al.* GPCP's new land surface precipitation climatology based on
1575 quality-controlled in situ data and its role in quantifying the global water cycle. *Theor.*
1576 *Appl. Climatol.* **115**, (2014).
- 1577 257. Funk, C. *et al.* The climate hazards infrared precipitation with stations - A new
1578 environmental record for monitoring extremes. *Sci. Data* **2**, (2015).
- 1579 258. Gedney, N., Huntingford, C., Comyn-Platt, E. & Wiltshire, A. Significant feedbacks of
1580 wetland methane release on climate change and the causes of their uncertainty.
1581 *Environ. Res. Lett.* **14**, (2019).
- 1582 259. Best, M. J. *et al.* The Joint UK Land Environment Simulator (JULES), model
1583 description – Part 1: Energy and water fluxes. *Geosci. Model Dev.* **4**, (2011).
- 1584 260. Clark, D. B. *et al.* The Joint UK Land Environment Simulator (JULES), model
1585 description – Part 2: Carbon fluxes and vegetation dynamics. *Geosci. Model Dev.* **4**,
1586 (2011).
- 1587 261. Huntingford, C. *et al.* IMOGEN: An intermediate complexity model to evaluate
1588 terrestrial impacts of a changing climate. *Geosci. Model Dev.* **3**, (2010).

- 1589 262. Huntingford, C. & Cox, P. M. An analogue model to derive additional climate change
1590 scenarios from existing GCM simulations. *Clim. Dyn.* **16**, (2000).
1591
1592
1593

1594 **BOX 1: Physical geography of Eastern Africa**

1595

1596 The physical geography of Eastern Africa is relevant to the dynamics of rainfall weather
1597 systems^{49,251} and to the subsequent surface movement of water (see figure). The region is
1598 dominated by the East African Rift, running from the Afar Triple Junction near the Red Sea
1599 southwards through Eastern Africa to Mozambique that also produces the Ethiopian and
1600 Kenyan Highlands.

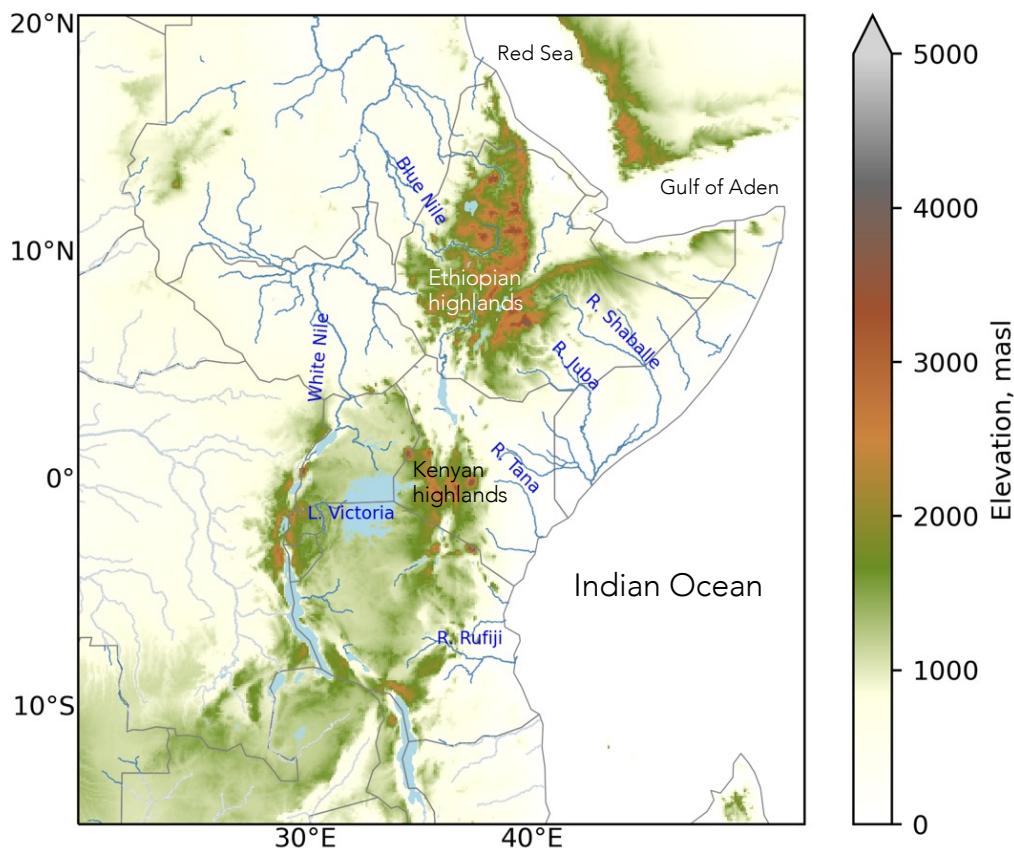
1601

1602 Eastern Africa is dominated by the Nile River basin but also encompasses tributaries of the
1603 Congo as well several regionally important rivers draining eastwards into the Red Sea, the
1604 Gulf of Aden and the Indian Ocean. Two endorheic rivers, the Awash and Omo, terminate in
1605 the Afar depression and Lake Turkana, respectively. The Nile Basin includes several rift valley
1606 lakes including Lake Victoria which collects water from Burundi, Rwanda, northern Tanzania,
1607 and the Kenyan Highlands and has an important role in regulating flows in the White Nile
1608 downstream.

1609

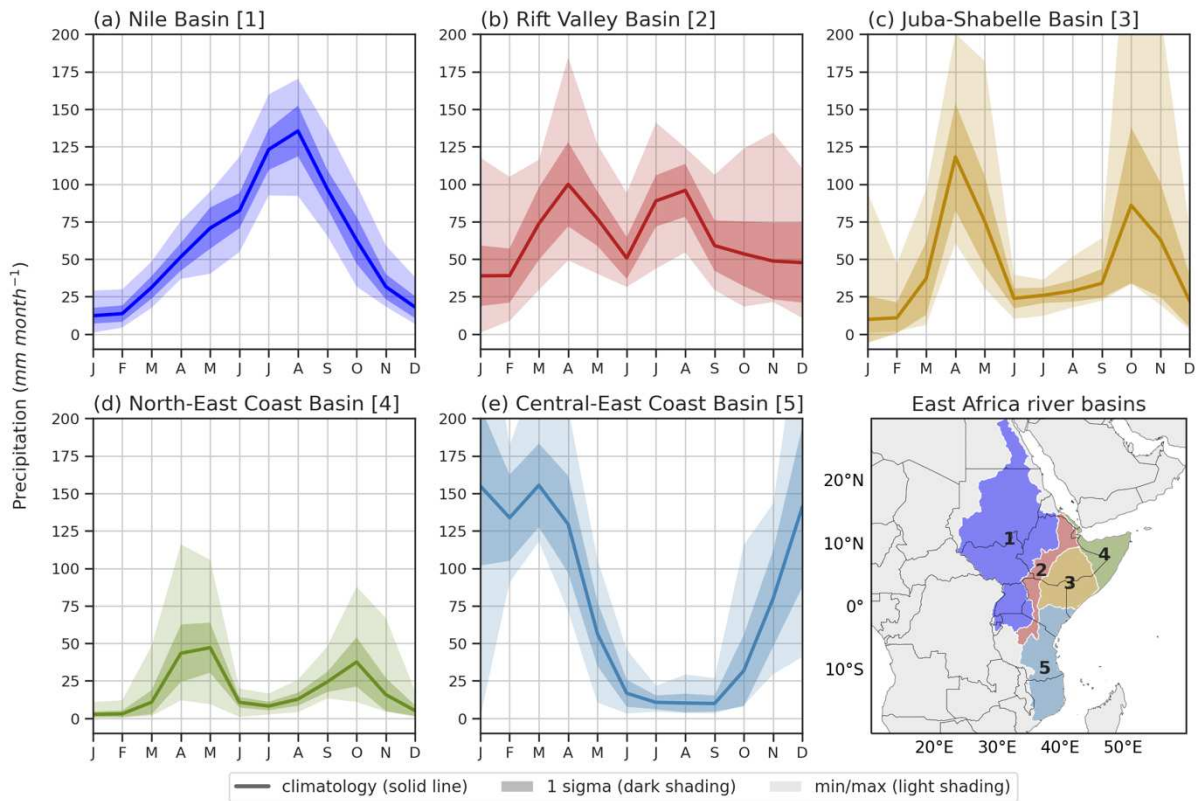
1610 Tributaries draining the western Ethiopian highlands bring additional seasonal flows (during
1611 August-October) with the largest of these, the Blue Nile, joining at Khartoum to form the main
1612 river Nile²⁵². Lake Kivu and Lake Tanganyika and its tributaries in western Tanzania form the
1613 headwaters of the Congo²⁵³. Watersheds east and south of the Ethiopian highlands and
1614 eastern rift valley flow into the Indian Ocean, providing an essential source of water to
1615 populations in more arid coastal plains, for example Shabelle and Juba in Somalia. In addition
1616 to the rift valley lakes, areas of extensive seasonal flooding, for example the Sudd in South
1617 Sudan, lead to significant water losses to the atmosphere by evaporation¹²⁹.

1618



1619

1620

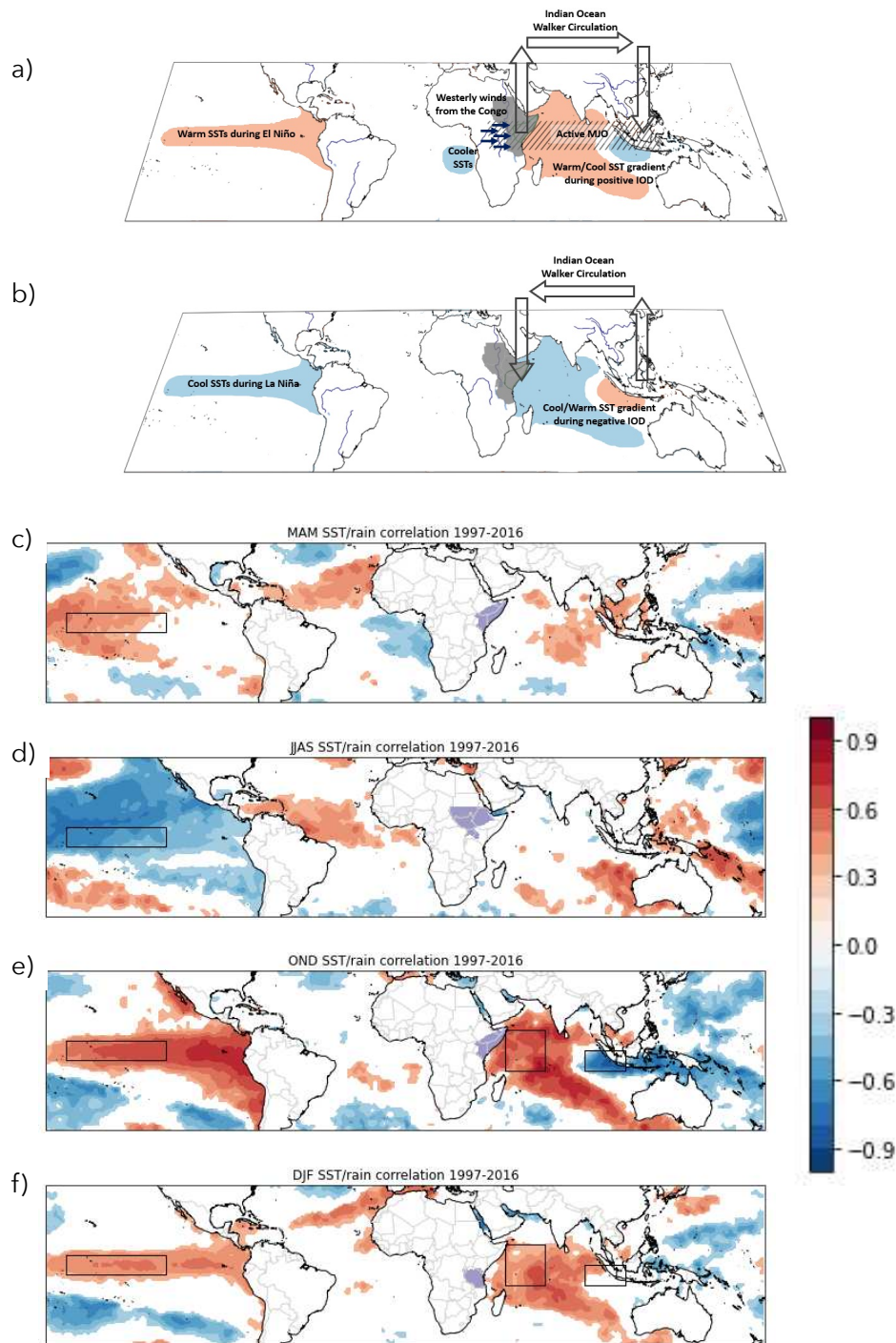


1622

1623 **Figure 1 Seasonal cycle of area-mean rainfall across five river basins (a-e) across**
 1624 **Eastern Africa (f), 1983-2019. a]** Mean seasonal rainfall in the Nile Basin (area 1 in the map,
 1625 as delineated by HydroBASINS²⁵⁴). The dark blue envelope denotes the standard deviation
 1626 about the monthly mean values and the light blue envelope the range of values. Values are
 1627 calculated from the monthly gridded gauge data from the Global Precipitation Climatology
 1628 Centre (GPCC)^{255,256}. **b]** As in a, but for the Rift Valley Basin (area 2 in the map). **c]** As in a,
 1629 but for the Juba-Shabelle Basin (area 3 in the map). **d]** As in a, but for the North-East Coast
 1630 Basin (area 4 in the map). **e]** As in a, but for the Central-East Coast Basin (area 5 in the map).
 1631 Substantial differences in the magnitude, variation and (bimodal) seasonal cycle of rainfall are
 1632 evident across Eastern Africa.

1633

1634



1635

1636

1637

1638

1639

1640

1641

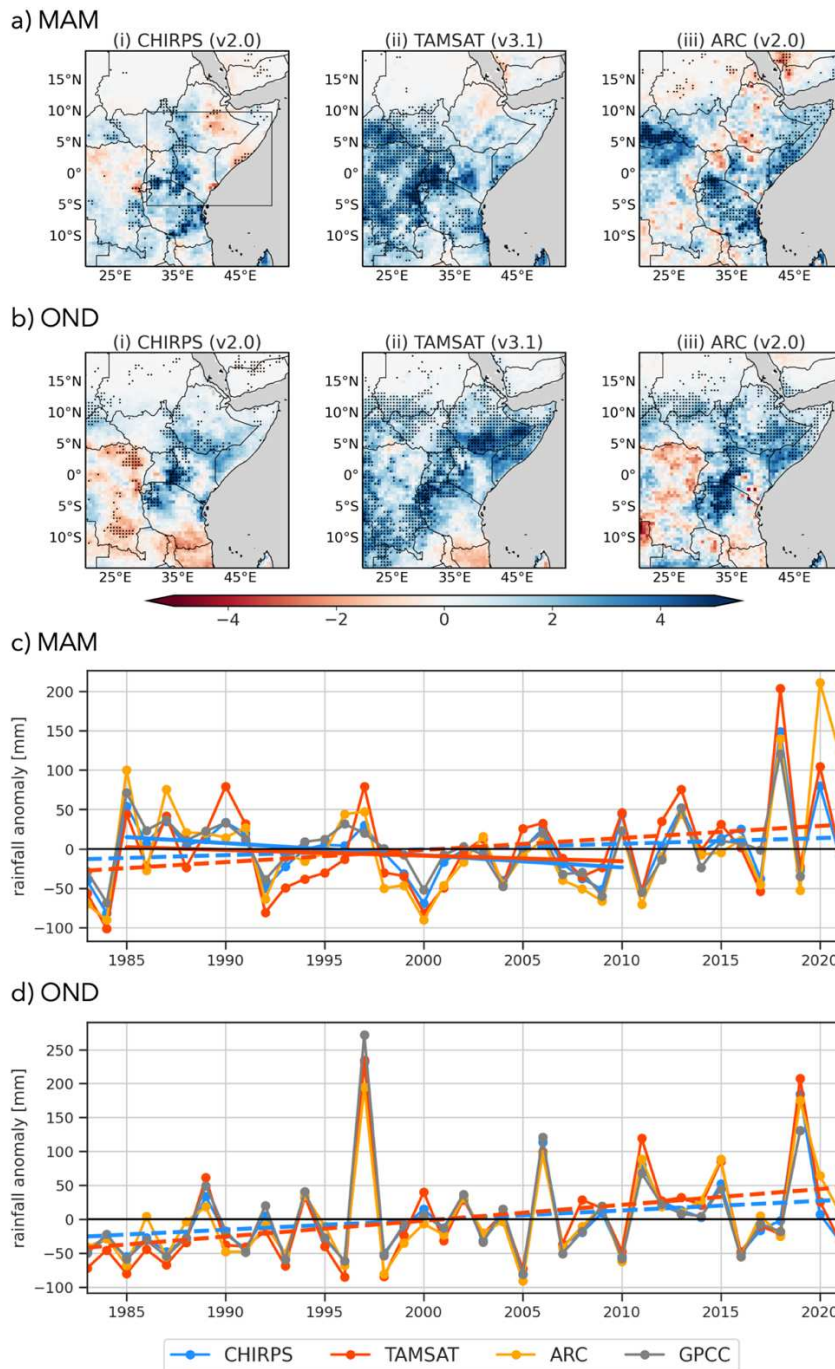
1642

1643

1644

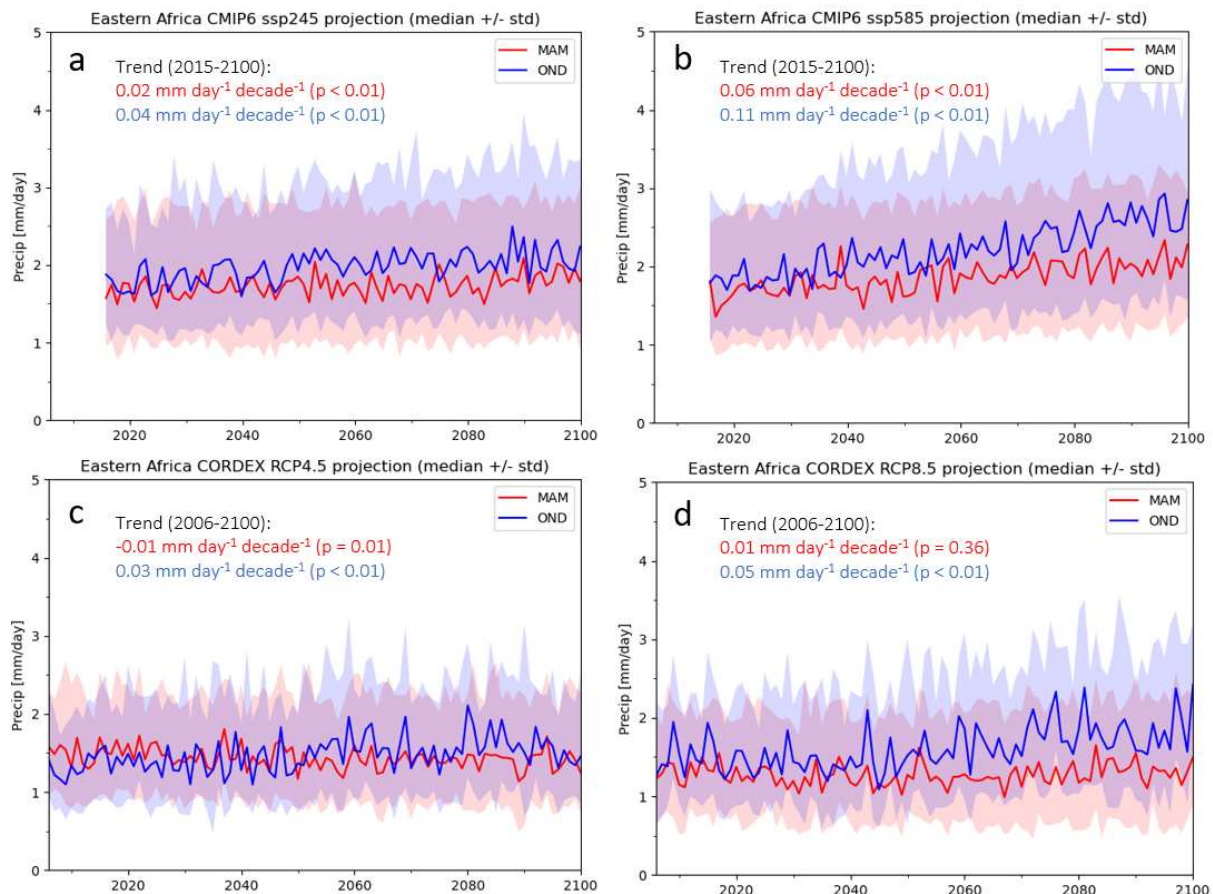
1645

Figure 2 **the main physical processes that determine rainfall variations over Eastern Africa.** a) mechanisms that lead to enhanced rainfall over Eastern Africa. Orange and blue shading denotes warm and cool sea surface temperatures (SSTs), respectively b) Mechanisms that lead to reduced rainfall over Eastern Africa. Rainfall variations are determined by processes that act on local spatial scales and via atmospheric teleconnections. The green contour marks the region that experiences a bimodal regime. c-f) seasonal correlations between SST and regional Eastern African rainfall (denoted by areas with purple shading). Black open rectangles over the Pacific and Indian Ocean define the regions we use to calculate the ENSO and IOD.



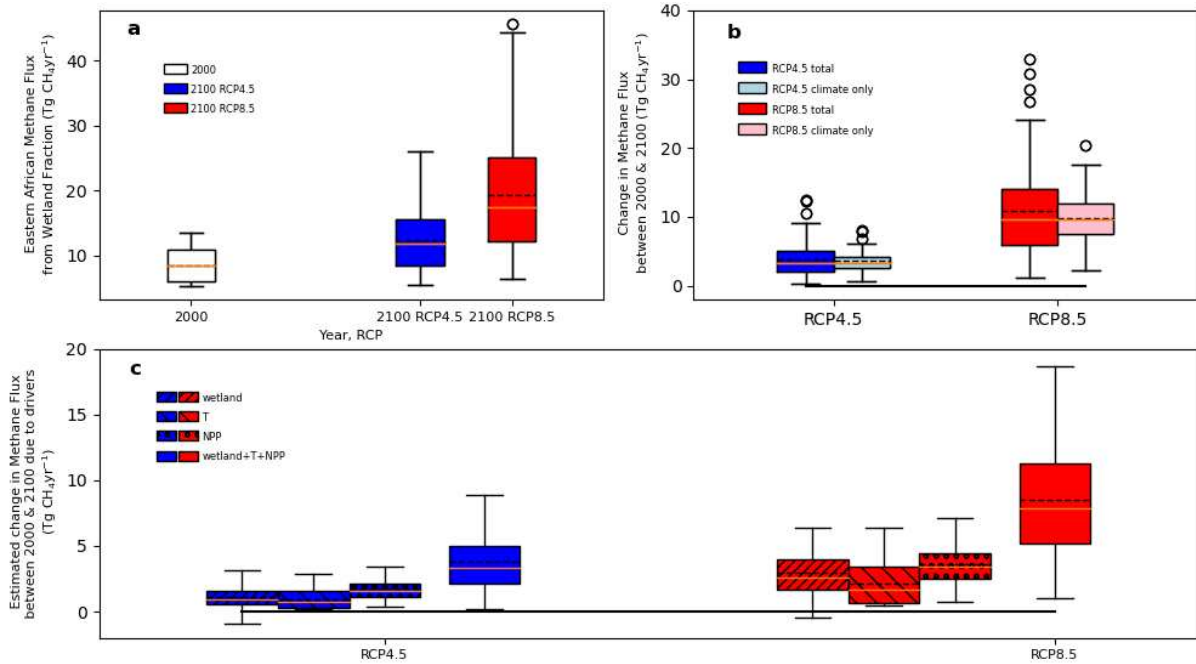
1646
 1647
 1648
 1649
 1650
 1651
 1652
 1653
 1654
 1655
 1656
 1657
 1658

Figure 3 Spatial and temporal variations of rainfall over Eastern Africa. a) mean rainfall trends during the long rains (MAM) over 1983-2021 for three datasets: CHIRPS²⁵⁷ (top left); TAMSAT⁴⁰ (top middle); and ARC⁸⁴ (top right). Stippling denotes statistically significant trends at the 95% confidence level using the Wald test. b) as in a, but for the short rain (OND). c) area-weighted total rainfall anomalies during MAM over part of Eastern Africa (30-50°E, 5°S-10°N; see box in top left panel of a) for the three datasets, including GPCC. Anomalies are calculated relative to the 1983-2021 monthly means. d) As in c, but for OND. Dashed and solid lines denote linear trend lines for CHIRPS and TAMSAT over periods 1983-2021 and 1985-2010, respectively, with colours corresponding to the data; the shorter period is used to highlight changes in the long rains in the 1990s. There is better agreement between trends determined by different rainfall data products for the short rains.



1659
 1660
 1661
 1662
 1663
 1664
 1665
 1666
 1667

Figure 4 Projections of long rains and short rains. a) Multi-model median long rain (MAM; red) and short rain (OND; blue) projections from CMIP6 models forced under SSP 2-4.5. Shading denotes the standard deviation associated with the ensemble of model runs. b) As in a, but for CMIP6 models forced under SSP 5-8.5. c) Multi-model median long rain (MAM; red) and short rain (OND; blue) projections from CORDEX regional climate models forced with RCP4.5. d) As in c, but for CORDEX regional climate forced with RCP8.5. Global and regional climate model projections suggest that short rain totals will exceed those of the long rains, the timing of which depends on the future scenario.



1668

1669

1670

1671

1672

1673

1674

1675

1676

1677

1678

1679

1680

1681

Figure 5 Wetland methane emission over Eastern Africa. **a)** methane emission estimates from the JULES model for 2000 (white) and 2100 driven by RCP4.5 (blue) and RCP8.5 (red). **b)** changes in methane emission estimates between 2000 and 2100 for RCP4.5 and RCP8.5. Spread, denoting climate uncertainty, is shown by light blue (RCP4.5) and pink (RCP8.5) box and whiskers. **c)** linearised estimates of changes to methane emissions from 2000 to 2100 under RCP4.5 and RCP8.5²⁵⁸ owing to inundation extent, soil temperature, NPP and inundation extent + soil temperature + NPP. In all cases, boxes describe the interquartile range (IQR), the whiskers the quartiles $\pm 1.5 \times$ IQR, circles outliers, and the orange and dashed black lines the mean and median values, respectively, associated with the ensemble of model runs. Future increases in methane emissions are driven approximately equally by warmer temperature, higher rainfall and larger NPP. The solid horizontal lines in b and c denote the zero line.

1682 **Supplementary Information << new file >>**

1683

1684 To understand the response of wetland methane emissions over Eastern Africa to future
1685 climate output from the JULES land surface model^{259,260} is analysed, coupled with the
1686 IMOGEN impacts model^{258,261}. IMOGEN is calibrated against 34 different CMIP5 ESM-based
1687 climate simulations where the climate is described using pattern-scaling²⁶².

1688

1689 Fitted to the climate projection from each ESM, IMOGEN assumes a linear relationship at
1690 each grid-box and for each month between changes in meteorology and global warming, itself
1691 a function of atmospheric radiative forcing. The IMOGEN system allows an exploration of the
1692 uncertainty in the climate projections and the wetland methane emission models. The JULES
1693 wetland methane emissions model is driven by wetland extent, available substrate, and soil
1694 temperature.

1695

1696 In this analysis net primary productivity as a surrogate for the substrate²⁵⁸. Ranges of regional
1697 totals are used to described wetland model uncertainty, based on the best current global
1698 totals²⁵⁸ and a range of temperature sensitivities²⁵⁸.

1699